The prion protein is an agonistic ligand of the G protein-coupled receptor Adgrg6

Küffer, Alexander ; Lakkaraju, Asvin K K ; Mogha, Amit ; Petersen, Sarah C ; Airich, Kristina ; Doucerain, Cédric ; Marpakwar, Rajlakshmi ; Bakirci, Pamela ; Senatore, Assunta ; Monnard, Arnaud ; Schiavi, Carmen ; Nuvolone, Mario ; Grosshans, Bianka ; Hornemann, Simone ; Bassilana, Frederic ; Monk, Kelly R ; Aguzzi, Adriano

Abstract: Ablation of the cellular prion protein PrPC leads to a chronic demyelinating polyneuropathy affecting Schwann cells. Neuron-restricted expression of PrPC prevents the disease1, suggesting that PrPC acts in trans through an unidentified Schwann cell receptor. Here we show that the cAMP concentration in sciatic nerves from PrPC-deficient mice is reduced, suggesting that PrPC acts via a G protein-coupled receptor (GPCR). The amino-terminal flexible tail (residues 23–120) of PrPC triggered a concentration-dependent increase in cAMP in primary Schwann cells, in the Schwann cell line SW10, and in HEK293T cells overexpressing the GPCR Adgrg6 (also known as Gpr126). By contrast, naive HEK293T cells and HEK293T cells expressing several other GPCRs did not react to the flexible tail, and ablation of Gpr126 from SW10 cells abolished the flexible tail-induced cAMP response. The flexible tail contains a polycationic cluster (KKRPKPG) similar to the GPRGKPG motif of the Gpr126 agonist type-IV collagen2. A KKRPKPG-containing PrPC-derived peptide (FT23–50) sufficed to induce a Gpr126-dependent cAMP response in cells and mice, and improved myelination in hypomorphic gpr126 mutant zebrafish (Danio rerio). Substitution of the cationic residues with alanines abolished the biological activity of both FT23–50 and the equivalent type-IV collagen peptide. We conclude that PrPC promotes myelin homeostasis through flexible tail-mediated Gpr126 agonism. As well as clarifying the physiological role of PrPC, these observations are relevant to the pathogenesis of demyelinating polyneuropathies—common debilitating diseases for which there are limited therapeutic options.

DOI: https://doi.org/10.1038/nature19312

The prion protein is an agonistic ligand of the G protein-coupled receptor Gpr126/Adgrg6

Alexander Küffer[1,*], Asvin KK Lakkaraju[1,*], Amit Mogha[2], Sarah C. Petersen[2], Kristina Airich[1], Cédric Doucerain[1], Rajlakshmi Marpakwar[1], Pamela Bakirci[1], Assunta Senatore[1], Arnaud Monnard[1], Carmen Schiavi[1], Mario Nuvolone[1], Bianka Grosshans[3], Simone Hornemann[1], Frederic Bassilana[3], Kelly R. Monk[2], and Adriano Aguzzi[1,†]

[1] Institute of Neuropathology, University of Zurich, CH-8091 Zürich, Switzerland

[2] Washington University School of Medicine, Department of Developmental Biology and Hope Center for Neurological Disorders, 660 South Euclid Avenue, Campus Box 8103, St. Louis, MO 63110

[3] Novartis Institutes of Biomedical Research, CH-4056 Basel, Switzerland

* Equal contribution

[†]Corresponding author:

Adriano Aguzzi, Institute of Neuropathology, University of Zurich

Schmelzbergstrasse 12, CH-8091 Zurich, Switzerland

Tel: +41-44-255-2107, Email: adriano.aguzzi@usz.ch

Ablation of the cellular prion protein PrP^C leads to a chronic demyelinating polyneuropathy (CDP) affecting Schwann cells. Neuron-restricted PrP^C expression prevents the disease[1], suggesting that it acts in *trans* through an unidentified Schwann cell receptor. We found that the cAMP concentration in PrP^C-deficient sciatic nerves is reduced, suggesting the involvement of a G protein-coupled receptor (GPCR). The amino-terminal "flexible tail" (FT, residues 23-120) of PrP^C triggered a concentration-dependent cAMP increase in primary Schwann cells, in the Schwann-cell line SW10, and in Hek293T cells overexpressing the GPCR Gpr126/Adgrg6. In contrast, naïve HEK293T cells and HEK293T cells expressing several other GPCRs did not react to the FT, and ablation of Gpr126 from SW10 cells abolished the FT-induced cAMP response. The FT contains a polycationic cluster (KKRPKPG) similar to the GPRGKPG motif of the Gpr126 agonist, type-IV collagen[2] (Col4). A KKRPKPG-containing PrP^C-derived peptide (FT_{23-50}) sufficed to induce a Gpr126-dependent cAMP response in cells and mice, and improved myelination in hypomorphic Gpr126 zebrafish mutants. Substitution of the cationic residues with alanines abolished the biological activity of both FT_{23-50} and the respective Col4 peptide. We conclude that PrP^C promotes myelin homeostasis through FT-mediated Gpr126 agonism. Besides clarifying the physiological role of PrP^C, these observations are relevant to the pathogenesis of demyelinating polyneuropathies, common debilitating diseases with limited therapeutic options.

Neuronal *Prnp* ablation triggers CDP[1], suggesting the existence of a PrP^C receptor on Schwann cells. We therefore assessed the binding of full-length PrP^C (recPrP, residues 23-231), FT (residues 23-110), or its refolded globular domain (GD, residues 121-231), to primary Schwann cell cultures (PSC) from $Prnp^{ZH1/ZH1}$ sciatic nerves[3] using POM1 and POM2 antibodies[4]. Both recPrP and FT, but not GD, were found to stain PSC (**Fig. S1A**).

Using transcription activator-like effector nucleases, we generated a *Prnp*-ablated subclone (termed $SW10_{\Delta PrP}$) of the SW10 Schwann-cell line (**Fig. S1B-C**). Again recPrP and FT, but not GD, adhered to $SW10_{\Delta PrP}$ cells (**Fig. 1A, S1D-E**). Neither recPrP nor FT adhered to the $Prnp^{-/-}$ hippocampal cell line HpL[5] (**Fig. S1F**), suggesting that binding was specific to Schwann cells. We next measured the binding of synthetic PrP-derived peptides (2 µM, 20 min) to $SW10_{\Delta PrP}$ cells (**Fig. 1B**). FT_{23-50}, but neither FT_{39-66} nor

any of the carboxy-proximal peptides (**Table S1**), showed binding (**Fig. 1C**) suggesting that residues 23-38 are essential for the interaction.

We treated SW10 cells with trypsin (2.5% w/v, 10 min) in order to degrade membrane-resident proteins. Following trypsin inactivation, we added non-trypsinized SW10 cells labeled with the cell-tracking dye Deep Red. HA-tagged FT_{23-50} (2µM) was added, and binding was monitored with anti-HA antibodies. 51% of non-trypsinized cells and 5% of trypsinized cells showed FT_{23-50} binding (**Fig. S1G**), suggesting the existence of a surface FT receptor on Schwann cells. Cytofluorimetry revealed no altered binding of HA-tagged FT_{23-50} to SW10 cells treated with phosphoinositol phospholipase C (PI-PLC, 30' at 37°C), indicating that binding did not require GPI-anchored surface proteins, whereas binding of POM2 was greatly reduced indicating that PrP^C had been stripped from cell surfaces (**Fig. S1H**).

Might the FT alter cAMP signaling in Schwann cells? At 4 days of age, $Prnp^{ZH1/ZH1}$ and WT sciatic nerves showed similar cAMP levels (**Fig. S2A**). At 4 weeks of age, $Prnp^{ZH1/ZH1}$sciatic nerves showed a trend towards decreased cAMP levels (**Fig. S2B**). At 12-16 weeks, when CDP is incipient in $Prnp^{ZH1/ZH1}$mice[1], $Prnp^{ZH1/ZH1}$ nerves exhibited significantly lower cAMP levels (**Fig. 1D**, p=0.0115). Strictly isogenic C57BL/6J $Prnp^{ZH3/ZH3}$ (ref. 6); sciatic nerve lysates from these mice (10-16 week old) also displayed significantly lower levels of cAMP than wild-type mice (**Fig. S2C**).

Sciatic nerves from 12-16 week old *tg*NSE-PrP mice, expressing PrP^C in neurons, showed cAMP levels similar to wild-type mice, whereas *tg*MBP-PrP sciatic nerves, which express PrP^C in Schwann cells and suffer from CDP[1], showed lower cAMP levels (**Fig. 1E**). Moreover, when treated with FT (0.1-5 µM; 20 min), $Prnp^{ZH1/ZH1}$ PSC and SW10 cells displayed a concentration-dependent cAMP increase (**Figs. 2A, S2D**) with an EC_{50} of 860 nM (**Fig. 2B**).

We transfected HEK293T cells, which express little endogenous PrP^C, with a plasmid expressing murine PrP^C or with an empty plasmid (HEK^{PrP} and HEK^{empty}, respectively). Immunoprecipitations showed that HEK^{PrP} cells released soluble FT (ca. 37 ng FT/ml, **Fig. S3A-B**). Exposure to conditioned medium from HEK^{PrP} cells, but not from HEK^{empty} cells, raised cAMP levels in PSC cultures generated from $Prnp^{ZH1/ZH1}$ mice (**Fig. 2C**). Spent medium from PSC cultures and sciatic nerves from 10-week old C57BL/6 mice did not contain any FT, suggesting that little FT is released by Schwann cells (**Fig. S3C-D**)

To assess if the FT contains motifs responsible for inducing the cAMP response, we treated $SW10_{\Delta PrP}$ cells with the same synthetic peptides previously used to assess binding to Schwann cells. Peptide FT_{23-50} induced cAMP, whereas FT_{34-69} and all carboxy proximal peptides were inactive (**Fig. 2D**). These results suggest that residues 23-33, which contain the lysine-rich "charge cluster 1" (CC1), represent the biologically active region of the FT. To test the latter prediction, we incubated FT_{23-50} with monovalent recombinant phage-derived miniantibodies recognizing the CC1 (Fab3) or the octapeptide repeats (Fab71) of PrP^{C}. Preincubation with Fab3, but not with Fab71, significantly quenched the ability of FT_{23-50} to induce cAMP in $SW10_{\Delta PrP}$ cells (**Fig. 2E**).

Peripheral nervous system myelination is controlled by Gpr126, an adhesion GPCR expressed by Schwann cells[7,8]. We therefore generated HEK293T cells stably overexpressing human Gpr126 or, for control, Gpr124 and Gpr176 (denoted HEK^{Gpr126}, HEK^{Gpr124}, and HEK^{Gpr176}) with a C-terminal V5 epitope tag[9] (**Fig. S3E**). Flow cytometry revealed FT_{23-50} binding to HEK^{Gpr126} but neither to HEK^{Gpr124} nor to HEK^{Gpr176} cells (**Fig. 2F-S3F**). Moreover, FT_{23-50} exposure (20'; ≥500 nM) raised cAMP in HEK^{Gpr126} cells but not in HEK^{Gpr124} and HEK^{Gpr176} cells (**Fig. 3A**). We then treated HEK293T, HEK^{Gpr124}, and HEK^{Gpr126} cells with recombinant FT or GD (2µM, 20'). FT was detected only in HEK^{Gpr126} lysates immunoprecipitated with anti-V5 antibodies, and GD was never detected (**Fig. S4A**).

Next, we generated clonal SW10 cells devoid of endogenous Gpr126 (designated $SW10_{\Delta Gpr126}$). When treated with FT_{23-50}, SW10 (but not $SW10_{\Delta Gpr126}$) cells reacted with increased cAMP levels. A modified $FT^{K\rightarrow A}_{23-50}$ peptide (with lysine residues replaced with alanines) was ineffective in binding cells and inducing cAMP (**Fig. 3B**). We then treated $SW10_{\Delta Gpr126}$ cells transfected with human Gpr126, Gpr124, Gpr176 or Gpr56 with FT_{23-50}. Only Gpr126-transfected cells showed a cAMP response (**Fig. S4B**) similar to that of naïve SW10 cells, indicating that the tag did not affect the function of Gpr126 (**Fig. S4C**). When treated with conditioned media from HEK^{PrP} or HEK^{empty} cells, SW10 but not $SW10_{\Delta Gpr126}$ cells responded with a cAMP spike (**Fig. 3C**). Moreover, FT adsorption was reduced in $SW10_{\Delta Gpr126}$ cells (**Fig. S4D**).

We then administered FT_{23-50} (2µM, 20') to HEK^{Gpr126} cells and HEK293(H) cells transfected with plasmids encoding human Gpr56, Gpr64, Gpr133, or Gpr97. Only Gpr126-expressing cells showed a cAMP response (**Fig. S4E**). The magnitude of cAMP response was not enhanced by increasing the transfected plasmid, suggesting that other signaling components became limiting (**Fig. S4F**). There was no cAMP induction in

Prnp$^{ZH1/ZH1}$ cerebellar granule neuronal cultures treated with $FT_{23\text{-}50}$ or $FT^{K\rightarrow A}_{23\text{-}50}$ (**Fig. S5A**), as expected from the minimal Gpr126 expression in the brain[10]. The FT is released from PrP^C by metalloproteases[11]; after treatment with the metalloprotease inhibitor TAPI-2, HEK^{PrP}-conditioned medium contained significantly less FT (**Fig. S5B-C**) and displayed reduced cAMP-inducing activity (**Fig. S5B**).

Egr2/Krox-20 controls the expression of myelin genes and is implicated in myelin maintenance[12]. Egr2 expression was decreased in 13-week-old *Prnp*$^{ZH3/ZH3}$ sciatic nerves ($p<0.05$; **Fig. 3D**), and recombinant FT (2 µM, 24h) activated Egr2-dependent luciferase expression in SW10 cells (**Fig. S5D**). Similarly, *Egr2* transcription was upregulated in primary Schwann cells treated with recombinant FT (2 µM; 1h) (**Fig. S5E**). Also, Akt phosphorylation increased 5 min after treatment with recombinant FT (2µM) and peaked at 10 min in $SW10_{\Delta PrP}$ but not in $SW10_{\Delta Gpr126}$ cells (**Fig. S5F-G**). The integrity of SW10 cells and their subclones was confirmed by the expression of myelin genes (**Fig. S6A**).

We identified two regions of similarity between FT (KKRPKPG and QGSPG) and the Gpr126 ligand, Type-IV collagen (Col4)[2] (GPRGKPG and QGSPG, **Fig. 4A**). Replacement of the conserved cationic residues with alanines (KKRPKPG ⇨ AAAPAPG), but not other substitutions, abrogated cAMP induction in $SW10_{\Delta PrP}$ cells (**Fig. 4B**); treatment with $FT_{23\text{-}34}$ (2µM, 20'), which contains KKRPKPG, sufficed to induce cAMP in $SW10_{\Delta PrP}$ but not in $SW10_{\Delta Gpr126}$ cells (**Fig. 4C**). We next generated murine PrP^C mutants containing alanine substitutions in either of the two conserved motifs. After transient transfection, both mutants were highly expressed by HEK293T cells (**Fig. S6B**), and cleaved FT was recovered in the medium (**Fig. S6C**). When applied to $SW10_{\Delta PrP}$ cells, conditioned media from HEK293T cells expressing wild-type or QGSPG-mutated PrP^C ($HEK^{PrP}_{\sum QGSPG}$) induced cAMP, whereas medium from cells expressing KKRPK-mutated PrP^C ($HEK^{PrP}_{\sum KKRPK}$) did not (**Fig. S6D**). We then generated 21-mer peptides bearing the corresponding Col4 sequence (GPRGKPG) or an alanine-substituted variant (AAAGAAG). The native Col4 peptide (8 µM), but not the mutated peptide, induced cAMP in $SW10_{\Delta PrP}$ cells (**Fig. S6E**).

In zebrafish, Gpr126 controls myelination, yet *Prnp*$^{-/-}$ mice have no obvious myelination defects but develop a late-onset peripheral neuropathy with demyelination, onion bulb formation (**Fig. 5A, S7A**), decreased Remak bundles containing ≥10 axons and increased bundles containing <10 axons (**Fig. S7B**), indicative of impaired axon-Schwann cell interactions. To test if Gpr126 dysfunction may cause late-onset phenotypes in mice, we examined sciatic nerves from *Dhh*^{Cre}*::Gpr126*$^{fl/fl}$ mice experiencing Schwann-cell specific *Gpr126*

ablation from ~E12.5 onwards[13,14]. At one year of age, we noted neuropathic traits similar to those of *Prnp*$^{-/-}$ mice including reduced bundles containing >20 unmyelinated axons, increased bundles containing <10 axons, abnormal cytoplasmic Schwann cell protrusions[1] and onion bulbs (**Fig. 5B and S7C-D**).

The *gpr126*^{st63} zebrafish mutant has a point mutation reducing Gpr126 signaling and shows reduced myelin basic protein (Mbp) expression by Schwann cells of the posterior lateral line nerve (PLLn) (**Fig. 5C, S8A**) which can be rescued by Gpr126 activators[8,15,16]. When applied to *gpr126*^{st63} zebrafish larvae at 50-55h post-fertilization (hpf), $FT_{23\text{-}50}$ (20 µM) increased Mbp expression in the PLLn at 5 days post-fertilization (dpf) compared to DMSO-treated larvae (**Fig. 5C-5D**, $p<0.05$). We also treated *gpr126*^{st49} larvae, which encode a truncated Gpr126 incapable of G_s signaling[8,16]. Mbp was barely detectable in both $FT_{23\text{-}50}$ and DMSO-treated mutant *gpr126*^{st49} larvae (**Fig. 5C, S8B**).

We next administered intravenous $FT_{23\text{-}50}$ or $FT^{K\rightarrow A}_{23\text{-}50}$ peptide (600 µg) to 10-16 week old *Prnp*$^{ZH3/ZH3}$ and wild-type mice (N=8 per group, all littermates). $FT_{23\text{-}50}$, but not $FT^{K\rightarrow A}_{23\text{-}50}$, induced cAMP elevation in both *Prnp*$^{ZH3/ZH3}$ and *Prnp*$^{ZH1/ZH1}$ sciatic nerves 20 minutes post injection; cAMP reached levels similar to those of BL6 mice injected with $FT^{K\rightarrow A}_{23\text{-}50}$ (**Fig. 5E, S8C**). $FT_{23\text{-}50}$ induced a cAMP spike also in the heart, which expresses Gpr126 (**Fig. 5F, S8D**) but not in kidney and brain (**Fig. S8E-F**) which do not express Gpr126[17]. Finally, $FT_{23\text{-}50}$ but not $FT^{K\rightarrow A}_{23\text{-}50}$ (600 µg) induced a robust cAMP spike in *Gpr126*$^{fl/fl}$ but not in *Dhh*^{Cre}*::Gpr126*$^{fl/fl}$ sciatic nerves (**Fig. 5G**).

Here we report the first molecular elucidation of a phenotype caused by PrP^C deficiency. While Gpr126 is crucial for peripheral nerve myelination during development, the late-onset phenotype of *Prnp*-ablated mice suggests additional roles in myelin maintenance. While *Gpr126*$^{-/-}$ mice exhibit drastic hypomyelination, the *Prnp*$^{-/-}$ phenotype is relatively mild and late-onset akin to peripheral neuropathies, whose prevalence is 2.4% generally and 8% among the aged[18]. Perhaps Gpr126 provides basal signaling in *Prnp*$^{-/-}$ mice through its interaction with type-IV collagen and/or laminin-211 (ref. 2,16), which may not suffice for long-term myelin maintenance. The Gpr126-agonistic properties of systemically administered FT peptides suggests that soluble ligands may be beneficial in diseases caused by hypomorphic Gpr126 mutations[19], and perhaps also in other hereditary motor-sensory neuropathies.

A moderately conserved homology region between PrP^C and Col4 proved essential to the biological activity of both proteins, whereas laminin-211 may activate Gpr126 through different mechanisms. Although Gpr126 is not expressed in the central nervous system, certain mutants of PrP^C cause myelin pathology in vivo[20]. This observation raises the question whether inappropriate GPCR activation may play a role in prion diseases within the CNS.

Methods

Mice

Mice were bred in specified-pathogen free facilities at the University Hospital Zurich and Washington University, and housed in groups of 3-5, under a 12 h light/12 h dark cycle (from 7 am to 7 pm) at 21±1°C, with sterilized chow (Kliba No. 3431, Provimi Kliba, Kaiseraugst, Switzerland) and water *ad libitum*. Animal care and experimental protocols were in accordance with the Swiss Animal Protection Law, and approved by the Veterinary office of the Canton of Zurich (permits 123, 130/2008, 41/2012 and 90/2013). The following mice were used in the present study: C57BL/6J, $Prnp^{ZH1/ZH1}$ (ref. 3), co-isogenic C57BL/6J $Prnp^{ZH3/ZH3}$ and $Prnp^{WT/WT}$ control mice[6] and Schwann cell-specifc $Dhh^{Cre};Gpr126^{fl/fl}$ mutants[3,4]. Mice of both genders were used for experiments unless specified. Archival tissues from previous studies[1,6] were also analyzed in the current study.

Primary Schwann cell culture

Sciatic nerves from postnatal day 2-5 were dissected using microsurgical techniques. Nerves were dissociated in serum-free DMEM supplemented with 0.05% collagenase IV (Worthington) for 1h in the incubator. Sciatic nerves were mechanically dissociated using fire-polished Pasteur pipettes. Cells were filtered in a 40 µM cell strainer and washed in Schwann cell culture medium (DMEM, Pen-Strep, Glutamax, FBS 10%) by centrifugation at 300g for 10 min. Resuspended cells were plated on 3.5 cm petri dishes previously coated with poly-L-lysine 0.01% (wt/vol) and laminin (1 mg/ml). Laminin (Cat. No: L2020; from Engelbreth-Holm-Swarm murine sarcoma basement membrane) and poly-L-lysine were obtained from Sigma-Aldrich.

Purification of recombinant proteins

Full-length recombinant PrP (recPrP, residues 23-231) and globular domain (GD, residues 121-231) were purified as previously described[21-23]. The generation of the GST fusion FT-PrP expression vector (pGEX-KG FT-PrP) was described previously; a modified purification protocol was used[24]. The FT-PrP expression vector was transformed into BL21 (DE3) strain of Escherichia coli (Invitrogen). Bacteria were grown in Luria-Bertani medium to an OD of 0.6, and the expression of the fusion protein was induced with 0,5mM isopropyl-1-thio-β-D-galactopyranoside (AppliChem). Cells were then grown for another 4h at 37 °C and

100 rpm shaking. Cells were pelleted at 5000g for 20 min at 4 °C (Sorvall centrifuge, DuPont). The pellet was resuspended on ice in lysis buffer (phosphate-buffered saline supplemented with complete protease inhibitors (EDTA-free, Roche), phenylmethyl sulfonyl fluoride (Sigma) and 150 µM lysozyme (Sigma) and incubated on ice for 30 min. Triton-X 100 (1%), $MgCl_2$ (10mM) and DNase I (5 µg/ml, Roche) were added, and the lysate was incubated on ice for 30 min. The lysate was than centrifuged for 20 min at 10'000g at 4°C. Glutathione sepharose beads were washed with PBS and incubated with the cell lysate for 1h at 4°C on a rotating device. Beads were packed into a column and washed with PBS until a stable baseline was reached as monitored by absorbance at A_{280} using an ÄKTAprime (GE healthcare). The fusion protein was cleaved on the beads with 5U/ml Thrombin (GE Healthcare) for 1h at room temperature under agitation. For thrombin removal, benzamidine sepharose beads were added and incubated for 1h at 4°C on a rotating wheel. Protein preparations were analyzed by 12% NuPAGE gels followed by Coomassie- or silver-staining. To achieve a higher purity of the protein, we next applied the protein to a sulphopropyl (SP) sepharose column equilibrated with 50mM Tris-HCl buffer, pH=8.5. Elution was performed with a linear NaCl gradient ranging from 0–1000 mM. Fractions containing the protein were collected and concentrated (AMICON; MWCO 3500). The protein was then injected in 500 µl portions into a size-exclusion chromatography system (TSK-GEL $G2000SW_{XL}$ column (Tosoh Bioscience)) and eluted with a linear gradient using PBS. Pure fractions were combined, concentrated and stored at -20°C. The purity of FT-PrP was > 95-98 % as judged by a silver-stained 12% NuPAGE gel.

Cell Culture

SW10 cells and clones derived from it were all grown in DMEM medium supplemented with 10% fetal bovine serum (FBS), penicillin-streptomycin and Glutamax (all obtained from Invitrogen). HEK293T cells and clones derived therefrom were grown in DMEM-F12 medium supplemented with 10%FCS, penicillin-streptomycin and Glutamax (all obtained from Invitrogen). Human Gpr126 (NM_020455), Gpr124, Gpr64, Gpr56, Gpr133, Gpr56 and Gpr176 expression plasmids (pCGpr126-V5, pCGpr124-V5, pCGpr65-V5, pCGpr56-V5, pCGpr133-V5, pCGpr56-V5 and pCGpr176-V5) were generated by PCR amplification of the respective cDNA followed by TOPO cloning into the pCDNA3.1/V5-His-TOPO vector. The cDNA was in frame with the V5 tag (sequence: GKPIPNPLLGLDST) at the C terminus. HEK^{GPR126}, HEK^{GPR176} cells were generated by transfecting 1µg of plasmid in one well of a subconfluent 6-well plate using 3µl Fugene

(Roche) according to the manufacturer's protocol. 24h after transfection, cells were transferred to a 10cm dish and grown in selective medium containing 0.4 mg/ml G418 (Invitrogen) until emergence of resistant colonies. A limiting dilution was carried out to obtain clonal lines. Membrane expression of the transgene was assessed in the selected clones by confocal microscopy using 1:100 diluted anti-V5 antibody (Invitrogen) and the Cytofix/Cytoperm kit (Pharmingen Cat. Nr. 554714), according to manufacturer's protocol.

Cerebellar granule neuronal culture:

Cerebellar granule neurons were generated from 7-8 day old *Prnp*$^{ZH1/ZH1}$ mice with methods described previously[25]. Cultures were plated at 350,000 cells/cm^2 in Basal Medium Eagle (BME) (Invitrogen) with 10% (v/v) FCS and maintained at 37°C in 5% CO_2.

Plasmids and Transfections:

pCDNA-PrP^C was generated by cloning murine PrP^C into pCDNA3.1 vector as described previously [26]. Site-specific mutagenesis kit (Stratagene) was used to induce alanine substitutions of QPSPG and KKRPK domains in PrP^C. Primers used for generating Ala-QPSPG plasmid are: forward- GTG GAA GCC GGT ATC CCG GGG CGG CAG CCG CTG CAG GCA ACC GTT ACC C reverse: GGG TAA CGG TTG CCT GCA GCG GCT GCC GCC CCG GGA TAC CGG CTT CCA C. Primers for Ala-KKRPK are: forward- CTA TGT GGA CTG ATG TCG GCC TCT GCG CAG CGG CGC CAG CGC CTG GAG GGT GGA ACA CCG, reverse: CGG TGT TCC ACC CTC CAG GCG CTG GCG CCG CTG CGC AGA GGC CGA CAT CAG TCC ACA TAG. Transfections were performed with Lipofectamine 2000 (Invitrogen) according to manufacturer's protocol. 3µg of DNA was used per well of a 6-well plate. 24h post transfections, cells were washed using PBS, and fresh medium was added to the cells.

Immunoprecipitation

HEK293T and HEK^{GPR126} cells growing in T75 flasks at 50% density were treated with recombinant FT or GD (2µM, 20 min). Cells were washed twice in PBS and lysed in IP buffer: 1% Triton X-100 in PBS, 1x protease inhibitors (Roche) and Phospho stop (Roche) for 20 min on ice followed by centrifugation at 5000

rpm for 5 min at 4°C. BCA assays were performed to quantify the amount of protein, and 500 µg of protein was used for Immunoprecipitations. 2 µg of anti-V5 antibody were added to the cell lysate and incubated on a wheel rotator overnight at 4°C. On the following day, Protein G dynabeads (Invitrogen) were added to the samples and incubated for further 3h on the wheel at 4°C. Beads were washed three times, 5 min each using the IP buffer followed by addition of 2x sample buffer containing DTT (1mM final). Samples were heated at 95°C for 5 min, loaded on 4-12% Novex Bis-tris gels (Invitrogen), and migrated for 1.5h at 150V followed by western blotting. Immunoprecipitations were performed by adding 2 µg of POM2 antibody to 500µl of cell medium and incubating overnight on a wheel rotator at 4°C. Protein G beads were then added, and incubation on a wheel rotator at 4°C was performed again.

RNA Isolation and quantitative PCR

RNA extraction and quantitative PCR was performed as described previously[1]. The following primers were used: EGR2 fw: 5'-AATGGCTTGGGACTGACTTG-3'; EGR2 rev: 5'-GCCAGAGAAACCTCCATT-3' CA; GAPDH fw: 5'-CCACCCCAGCAAGGAGAC-3'; GAPDH rev: 5'-GAAATTGTGAGGGAGATGCT-3'.

Zebrafish mutant strains and analysis:

Adult zebrafish were maintained in the Washington University Zebrafish Consortium facility (http://zebrafishfacility.wustl.edu/) and all experiments were performed in compliance with institutional protocols. Embryos were collected from harem matings or *in vitro* fertilization, raised at 28.5°C, and staged according to standard protocols[27]. The *gpr126*^{st49} and *gpr126*^{st63} mutants were described previously[7,8].

Zebrafish peptide treatment, immunostaining, and quantification:

gpr126^{st63} or *gpr126*^{st49} mutants were collected from homozygous mutant crosses and WT larvae were collected from AB* strain crosses and raised to 50 hours post fertilization (hpf). FT_{23-50} treatment of *gpr126* mutants was performed as previously described[15]. Briefly, egg water was then replaced with either 20 µM FT_{23-50} in egg water or egg water containing an equivalent volume of DMSO. At 55 hpf, larvae were washed twice and raised in egg water to 5 days post fertilization (dpf). WT and *gpr126* larvae were fixed in 2%

paraformaldehyde + 1% tricholoroacetic acid in phosphate buffered saline, and Mbp and acetylated tubulin immunostaining was performed as described previously[8,28]. Expression scoring was performed with observer blind to treatment according to the following rubric: "strong" = strong and consistent expression throughout PLLn, "some" = weak but consistent expression in PLLn, "weak" = weak and patchy expression in PLLn, "none" = no expression in PLLn. N = three independent replicate *gpr126*^{st63} assays and one *gpr126*^{st49} assay. n = 87 DMSO-treated *gpr126*^{st63} larvae, 81 Prp-FT-treated *gpr126*^{st63} larvae, n = 27 DMSO-treated *gpr126*^{st49} larvae, n = 25 Prp-FT-treated *gpr126*^{st49} larvae.

Fluorescent nerve images were analyzed using the Fiji software[29]. A rectangle region-of-interest (ROI) was drawn longitudinally over the fluorescent nerve. The longitudinal grey-scale histogram of the myelin basic protein (MBP) was normalized pixel-by-pixel to the corresponding intensity of the acetylated tubulin (AcTub). The size of the measured ROIs was kept constant across different treatment modalities.

Flow cytometry

SW10 cells were grown in P75 flasks at 50% density, rinsed with PBS, and detached from culture flasks with dissociation buffer containing EDTA (GIBCO). After detaching, cells were washed to remove residual EDTA and counted using a Neubauer chamber. Batches of 10^5 SW10 cells were transferred to FACS tubes, treated with HA-tagged recombinant peptides for 20 minutes, washed, and incubated with Alexa-488 conjugated anti-HA antibody for 30 minutes. After further washes and centrifugations, cells were resuspended in 200µl of FACS buffer (PBS +10% FBS) and analyzed with a FACS Canto II cytofluorimeter (BD Biosciences). Data were analyzed using FloJo software.

Western blot analysis

Schwann cells were lysed in cell-lysis buffer (Tris-HCl 20mM, NaCl 137mM, Triton-X-100 1%) supplemented with protease inhibitor cocktail (Roche complete mini). The lysate was homogenized by passing several times through a 26G syringe, and cleared by centrifugation at 8000g, 4°C for 2 min. in a tabletop centrifuge (Eppendorf 5415R). Protein concentration was measured with the BCA assay (Thermo Scientific). 10 µg total protein was boiled in 4 x LDS (Invitrogen) at 95°C for 5 min. After a short centrifugation, samples were loaded on a gradient 4-12% Novex Bis-Tris Gel (Invitrogen) for electrophoresis

at constant voltage of 200V. Gels were transferred to PVDF membranes with the iBlot system (Life technologies). Membranes were blocked with 5% Top-Block (Sigma) in PBS-T for 1h at room temperature. Primary antibody was incubated overnight in PBS-T with 5% Top-Block. Membranes were washed three times with PBS-T for 10 min. and incubated for 1 hour with secondary antibodies coupled to horseradish peroxidase at room temperature. After three washes with PBS-T, the membranes were developed with Crescendo chemiluminescence substrate system (Millipore). Signals were detected using a Stella 3200 imaging system (Raytest, Straubenhardt, Germany).

Antibodies

Monoclonal antibodies against PrP^C were obtained and used as described previously[4]. Fab3 and Fab71 antibodies were generated using the phage display technology and their epitopes were mapped with overlapping peptides. Anti AKT, p-AKT were obtained from Cell signaling and used at 1:2000 dilutions for western blotting. Anti-p75NGF receptor antibody was obtained from Abcam and used at 1:200 dilutions for immunofluorescence. Anti V5 antibody was from Invitrogen and used at a dilution of 1:500 for western blot and 2µg of the antibody was used for immunoprecipitation on 500µg of cell lysate.

Cyclic AMP measurements

In the Direct cAMP ELISA assay, cAMP levels were assessed with a colorimetric competitive immunoassay (Enzo Life Sciences). Quantitative determination of intracellular cAMP was performed in cells or tissues lysed in 0.1 M HCl to stop endogenous phosphodiesterase activity and to stabilize the released cAMP. SW10 or HEK293T cells (100'000 cells /well) were plated in 6-well plates to a ca. 50% density. Cells were treated with conditioned media or recombinant peptides (2µM, unless specified) for 20 minutes unless otherwise mentioned. Cells were lysed with 0.1M HCl lysis buffer (Direct cAMP ELISA kit, Enzo). To ensure complete detachment of cells cell scrapers were used. Lysates were homogenized with 26G needle and syringe before clearing by centrifugation at 600g for 10 min. The subsequent steps were performed according to the manufacturer's protocol based on competition of sample cAMP with a cAMP-alkaline phosphatase conjugate. Cyclic AMP levels were calculated using a cAMP standard curve in the case of ELISA based assay. Finally, cAMP concentrations were normalized to total protein content in each sample.

cAMP changes are represented as fold changes to the respective controls. For each experiment, at least three independent biological replicates were used. For normalization purposes, the median value of the respective control sample was defined as "1". All measurements within each panel were normalized to this control value.

Generation of Schwann cell lines devoid of Gpr126

We designed two CRISPR short-guide RNA (sgRNAs) against exon 2 of Gpr126 (upper Guide CCTGTGTTCCTCTCTCAGGT and lower Guide AACAGGAACAGCAGGGCGCT). The DNA sequences corresponding to the sgRNAs were cloned into expression plasmids and transfected with EGFP-expressing Cas9-nickase plasmids. Single EGFP-expressing Schwann cells were isolated with a FACS sorter (Aria III). To determine the exact sequence of indels induced by genome editing we amplified the sgRNA-targeted locus by PCR and subcloned the fragments into blunt-TOPO vectors. Ten colonies per cell line were sequenced and showed distinct indels on each allele. A clonal subline devoid of Gpr126 was used for further studies. This cell line possessed insertions on both the alleles; a 49bp insertion at position 118 and a 5bp insertion at position 84 on each allele. Both insertions led to a frameshift and to the generation of premature stop codons leading to early translation termination.

Promoter luciferase assay

Luciferase reporter constructs were generated containing a 1.3kB sequence upstream of the transcription-starting site of Egr2. SW10 Schwann cells were transfected with Egr2 reporter construct and a renilla plasmid using lipofectamine 2000. After one day in vitro, Schwann cells were treated with recombinant full-length PrP (23-231), the globular domain of PrP (121-231) or PBS control. Luciferase activity was measured 24 hours after stimulation with Dual-Luciferase Reporter Assay System (Promega) according to the manufacturer's recommendations. Results were normalized to renilla transfection controls.

Immunocytochemistry

Glass coverslips were placed in 12-well plates (Thermo scientific) and coated with 0.01% wt/vol Poly-l-lysine solution (Sigma) overnight at room temperature. Coverslips were washed three times with ddH_2O and

dried for 2h in a laminar-flow hood. Schwann cells were seeded and cultured at 50% density. Cells were treated with recombinant FT-PrP, full length recPrP or C1-PrP for 20 min., and washed with serum-free DMEM. Cells were further washed with PBS followed by fixation with 4% paraformaldehyde. Fixed cells were incubated in blocking buffer (PBS+10%FBS) for 1h. Cells were treated with various primary antibodies followed by washes and incubation with Alexa 488 and Alexa 647 tagged rabbit or mouse secondary antibodies (Life technologies). Imaging was performed by Leica SP2 confocal microscope using a 20x objective; images were processed by Image J software.

Transmission electron microscopy

Transmission electron microscopy was performed as previously described[6]. Briefly, mice under deep anesthesia were subjected to transcardial perfusion with PBS heparin and sciatic nerves were fixed *in situ* with 2.5% glutaraldehyde + 2% paraformaldehyde in 0.1 M phosphate buffer, pH 7.4 and embedded in Epon. Ultrathin sections were mounted on copper grids coated with Formvar membrane and contrasted with uranyl acetate/lead citrate. Micrographs were acquired using a Hitachi H-7650 electron microscope (Hitachi High-Tech, Japan) operating at 80 kV. Brightness and contrast were adjusted using Photoshop. For quantification of Remak bundles and onion bulb like structures, images were captured at 1500X magnification and axon numbers and abnormal onion bulb like structures were counted manually. Quatification was performed in a blinded fashion by assigning numbers to the images and upon completion of quantification genotypes were revealed.

Recombinant peptides

HA-tagged and untagged synthetic peptides were produced by EZ Biosciences. A stock solution of 2mM was prepared by dissolving the peptides in PBS and they were used at a final concentration of 2μM unless specified. The sequences all the peptides used in this study can be found in Table S1.

References

1 Bremer, J. *et al.* Axonal prion protein is required for peripheral myelin maintenance. *Nat. Neurosci.* **13**, 310-318,(2010).

2 Paavola, K. J., Sidik, H., Zuchero, J. B., Eckart, M. & Talbot, W. S. Type IV collagen is an activating ligand for the adhesion G protein-coupled receptor GPR126. *Sci. Signal.* **7**, ra76,(2014).

3 Bueler, H. *et al.* Normal development and behaviour of mice lacking the neuronal cell-surface PrP protein. *Nature* **356**, 577-582,(1992).

4 Polymenidou, M. *et al.* The POM monoclonals: a comprehensive set of antibodies to non-overlapping prion protein epitopes. *PLoS One* **3**, e3872,(2008).

5 Kuwahara, C. *et al.* Prions prevent neuronal cell-line death. *Nature* **400**, 225-226,(1999).

6 Nuvolone, M. *et al.* Strictly co-isogenic C57BL/6J-Prnp-/- mice: A rigorous resource for prion science. *J. Exp. Med.* **213**, 313-327,(2016).

7 Pogoda, H. M. *et al.* A genetic screen identifies genes essential for development of myelinated axons in zebrafish. *Dev. Biol.* **298**, 118-131,(2006).

8 Monk, K. R. *et al.* A G protein-coupled receptor is essential for Schwann cells to initiate myelination. *Science* **325**, 1402-1405,(2009).

9 Kasof, G. M. & Gomes, B. C. Livin, a novel inhibitor of apoptosis protein family member. *J. Biol. Chem.* **276**, 3238-3246,(2001).

10 Zhang, Y. *et al.* An RNA-sequencing transcriptome and splicing database of glia, neurons, and vascular cells of the cerebral cortex. *J. Neurosci.* **34**, 11929-11947,(2014).

11 Altmeppen, H. C. *et al.* The sheddase ADAM10 is a potent modulator of prion disease. *Elife* **4**,(2015).

12 Decker, L. *et al.* Peripheral myelin maintenance is a dynamic process requiring constant Krox20 expression. *J. Neurosci.* **26**, 9771-9779,(2006).

13 Jaegle, M. *et al.* The POU proteins Brn-2 and Oct-6 share important functions in Schwann cell development. *Genes Dev.* **17**, 1380-1391,(2003).

14 Mogha, A. *et al.* Gpr126 functions in Schwann cells to control differentiation and myelination via G-protein activation. *J. Neurosci.* **33**, 17976-17985,(2013).

15 Liebscher, I. *et al.* A tethered agonist within the ectodomain activates the adhesion G protein-coupled receptors GPR126 and GPR133. *Cell Rep.* **9**, 2018-2026,(2014).

16 Petersen, S. C. *et al.* The adhesion GPCR GPR126 has distinct, domain-dependent functions in Schwann cell development mediated by interaction with laminin-211. *Neuron* **85**, 755-769,(2015).

17 Uhlen, M. *et al.* Proteomics. Tissue-based map of the human proteome. *Science* **347**, 1260419,(2015).

18 Ishida, C., Okino, S., Kitamoto, T. & Yamada, M. Involvement of the peripheral nervous system in human prion diseases including dural graft associated Creutzfeldt-Jakob disease. *J. Neurol. Neurosurg. Psychiatry* **76**, 325-329,(2005).

19 Kou, I. *et al.* Genetic variants in GPR126 are associated with adolescent idiopathic scoliosis. *Nat. Genet.* **45**, 676-679,(2013).

20 Radovanovic, I. *et al.* Truncated prion protein and Doppel are myelinotoxic in the absence of oligodendrocytic PrPC. *J. Neurosci.* **25**, 4879-4888,(2005).

21 Zahn, R., von Schroetter, C. & Wuthrich, K. Human prion proteins expressed in Escherichia coli and purified by high-affinity column refolding. *FEBS Lett.* **417**, 400-404,(1997).

22 Lysek, D. A. & Wuthrich, K. Prion protein interaction with the C-terminal SH3 domain of Grb2 studied using NMR and optical spectroscopy. *Biochemistry* **43**, 10393-10399,(2004).

23 Hornemann, S., Christen, B., von Schroetter, C., Perez, D. R. & Wuthrich, K. Prion protein library of recombinant constructs for structural biology. *FEBS J.* **276**, 2359-2367,(2009).

24 Guillot-Sestier, M. V., Sunyach, C., Druon, C., Scarzello, S. & Checler, F. The alpha-secretase-derived N-terminal product of cellular prion, N1, displays neuroprotective function in vitro and in vivo. *J. Biol. Chem.* **284**, 35973-35986,(2009).

25 Schulz, J. B., Weller, M. & Klockgether, T. Potassium deprivation-induced apoptosis of cerebellar granule neurons: a sequential requirement for new mRNA and protein synthesis, ICE-like protease activity, and reactive oxygen species. *J. Neurosci.* **16**, 4696-4706,(1996).

26 Dametto, P. *et al.* Neurodegeneration and unfolded-protein response in mice expressing a membrane-tethered flexible tail of PrP. *PLoS One* **10**, e0117412,(2015).

27 Kimmel, C. B., Ballard, W. W., Kimmel, S. R., Ullmann, B. & Schilling, T. F. Stages of embryonic development of the zebrafish. *Dev. Dyn.* **203**, 253-310,(1995).

28 Lyons, D. A. *et al.* erbb3 and erbb2 are essential for schwann cell migration and myelination in zebrafish. *Curr. Biol.* **15**, 513-524,(2005).

29 Schindelin, J. *et al.* Fiji: an open-source platform for biological-image analysis. *Nat. Methods* **9**, 676-682,(2012).

Acknowledgments

We thank Rita Moos, Petra Schwarz, Cinzia Tiberi, Christine Sturzenegger, Victor Escalante, Mirzet Delic, Charleen Johnson and Zachary Spence for technical help, Juliane Bremer for discussions, Valerie Beck, Marie Angela-Wulf, Karl Frontzek, Tory Johnson, Tracy O'Connor, Agnes Lau, and Claudia Rehwald for help in performing experiments, and Xianhua Piao for providing antibodies to Gpr126. AA is the recipient of an Advanced Grant of the European Research Council (Prion2020), a European Union Framework 7 Grant (NEURINOX), the Swiss National Foundation, the Clinical Research Priority Programs "Small RNAs" and "Human Hemato-Lymphatic Diseases", SystemsX.ch, and the Novartis Research Foundation. AL is supported by a grant of the Synapsis Foundation. SH is a recipient of SystemsX.ch grant. This work was supported by NIH grants F32 NS087786 to S.C.P. and NS079445 to K.R.M.

Author contributions:

AA, AK, KRM and AL designed experiments, analyzed data and wrote the manuscript. AK generated recombinant proteins, SW10ΔPrP and $SW10_{GPR126}$ cell lines, performed cAMP, q-PCR, FACS and luciferase assay. AL performed cAMP assays, IP, western blots, immunofluorescence, and FACS. CD contributed to immunofluorescence, extracted sciatic nerves from mice, performed intravenous injections and performed repetitions of cAMP and FACS assays. AM performed all Schwann-cell *Gpr126* mutant mouse experiments and SCP performed all zebrafish experiments, which were analyzed by AM, SCP, KRM, and AAG. RM performed cAMP assays, western blots, and FACS analyses. KA contributed to cAMP assays and western blots. PB performed the experiments in Fig. 1C and repeated cAMP assay for Fig. 5B-D. AS generated Fab3 and Fab71 antibodies. AM, CS, and KA contributed to Figures 2B, 2G, and 2A, respectively. MN generated ZH3 mice and performed electron microscopy. BG and FB generated GPR-overexpressing HEK cell lines. SH supervised generation of recombinant proteins, designed synthetic peptides, and contributed to writing the manuscript. All authors approved of the final version.

Competing Financial Interests: None

Figure Legends

Figure 1. Schwann cells selectively bind the flexible tail (FT) of PrP^C. **A**: *Prnp*-ablated SW10 cells ($SW10_{\Delta PrP}$) were exposed to recombinant PrP^C, FT, or GD ("ligand"). PrP^C and FT, but not GD, adhered to Schwann cells (red: POM1 and POM2 antibodies; grey: DAPI). $p75^{NGFR}$ antibodies identified Schwann cells. Scale bar: 26 µM. **B**: FT-derived peptides and PrP^C domains. CC1 and CC2: charge clusters 1 and 2. OR: octapeptide repeats. Peptides are color-coded as in panel C. **C:** $SW10_{\Delta PrP}$ cells were exposed to FT-derived peptides (2 µM; 20 min) carrying a carboxy-terminal hemagglutinin tag (HA). Flow cytometry showed strong binding by peptide FT_{23-50}. **D:** $Prnp^{ZH1/ZH1}$ sciatic nerves displayed lower cAMP than wild-type BL6 nerves. **E**: PrP^C expression by neurons (*tg*NSE-PrP), but not by Schwann cells (*tg*MBP-PrP), restored cAMP levels in sciatic nerves of 10-16 week-old mice. Dots: individual mice (11-15 mice/group). N.S.: non-significant. Error bars: standard error of the mean. Unpaired Student's t test was used for statistical analysis.

Figure 2. The FT fragment elicits a concentration-dependent cAMP response. **A**: Primary $Prnp^{ZH1/ZH1}$ Schwann cells were treated (20') with increasing concentrations of recombinant FT or with 10 µM GD. Ø: untreated cells. cAMP levels were determined in cell lysates ($5x10^5$ cells/assay). Addition of FT, but not of GD, induced a concentration-dependent cAMP response in Schwann cells. Here and henceforth: *: $p<0.05$; **: $p<0.01$; ***: $p<0.001$. **B**: Primary $Prnp^{ZH1/ZH1}$ Schwann cells (as described in A) were treated with FT (20'), and cAMP concentrations were determined by immunoassay. A dose-response curve was interpolated. **C**: cAMP concentrations in primary $Prnp^{ZH1/ZH1}$ Schwann cell cultures exposed to medium conditioned by HEK293T cells overexpressing wild-type murine PrP^C (HEK^{PrP}, right) or a non-coding vector (HEK^{empty}, left) as control. FT-containing medium resulted in cAMP induction. **D**: Synthetic peptides (27-44 residues) were added to $SW10_{\Delta PrP}$ cells (2 µM each, 20 min). Only FT_{23-50} induced cAMP. **E**: FT_{23-50} was preincubated with a two-fold molar excess of miniantibodies Fab3 or Fab71, and added to $SW10_{\Delta PrP}$ cells (20 min). Preincubation with Fab3, but not with Fab71, significantly quenched the FT-dependent cAMP spike. **F:** HA-tagged FT_{23-50} peptide (2µM) was added to wild-type HEK293T (HEK^{WT}) cells or to HEK^{GPR126} cells, labeled with anti-HA antibody, and subjected to cytofluorimetry. Overexpression of Gpr126 increased the binding of FT_{23-50}.

Figure 3. FT-dependent cAMP signaling in Gpr126-ablated Schwann cells. A: Intracellular cAMP in wild-type HEK293T cells and in Gpr176, Gpr124 and Gpr126 overexpressors exposed to $FT_{23\text{-}50}$ (0.5 µM, 20 min). Only HEK^{Gpr126} cells showed a cAMP increase. **B**: Wild-type (left) and Gpr126-ablated (right) SW10 cells were exposed to $FT_{23\text{-}50}$ (2µM, 20 min). SW10 cells, but not $SW10_{\Delta Gpr126}$ cells, respond to $FT_{23\text{-}50}$ with a cAMP spike. Moreover, SW10 cells did not respond to alanine-substituted $FT_{23\text{-}50}$ ($FT^{K\rightarrow A}_{23\text{-}50}$). **C**: SW10 and $SW10_{\Delta Gpr126}$ cells were incubated (20 min) with conditioned medium from HEK^{empty} or HEK^{PrP} cells.. HEK^{PrP}-conditioned medium induced a robust cAMP spike in SW10, but not $SW10_{\Delta Gpr126}$ cells. **D:** Protein was isolated from wild-type or $Prnp^{ZH3/ZH3}$ sciatic nerves (13-week old female mice) and Western blots were probed for EGR2 and actin. Densitometry (below) showed reduced Egr2 in $Prnp^{ZH3/ZH3}$ nerves (p=0.028).

Figure 4. FT and collagen-IV share a cAMP-inducing domain. A: Sequence alignment revealed two regions of similarity between the FT and Col4 (red boxes). Yellow and green shades represent high and moderate similarity, respectively. Dotted line: non-homologous residues. **B**: $SW10_{\Delta PrP}$ cells were treated with synthetic $FT_{23\text{-}50}$ or modified version of $FT_{23\text{-}50}$ in which the KKRPK or QGSPG motifs were replaced with alanines (2µM, 20'). Alanine substitution of KKRPK (peptide $FT^{K\rightarrow A}_{23\text{-}50}$), but not of QGSPG, abrogated cAMP induction. **C:** $SW10_{\Delta PrP}$ and $SW10_{\Delta Gpr126}$ cells were exposed (2µM, 20') to the synthetic peptides $FT_{23\text{-}50}$, $FT_{23\text{-}34}$ or $SFT_{23\text{-}34}$ (peptide containing scrambled amino acid sequence of $FT2_{3\text{-}34}$). $FT_{23\text{-}50}$ and $FT_{23\text{-}34}$ induced cAMP in $SW10_{\Delta PrP}$ cells but not $SW10_{\Delta Gpr126}$ cells.

Figure 5. Myelinotrophic effect of FT in zebrafish and mice.

A: Transmission electron micrographs from 14 month old wild-type BL6 and $Prnp^{ZH3/ZH3}$ sciatic nerves (*N*=3/4 animals). Thinly myelinated axons (arrowhead), loss of axon-Schwann cell interaction (boxes), abnormal cytoplasmic Schwann cell protrusions (white arrowhead) and initial onion bulb formation (asterisk) were observed in $Prnp^{ZH3/ZH3}$ mice. Scale bars: 500 nm. **B**: Neuropathic phenotype of one-year-old $Dhh^{Cre};Gpr126^{fl/fl}$ mutant mouse nerves. Left panels: toluidine blue-stained sections of sciatic nerves from control $Gpr126^{fl/fl}$ (phenotypically wild-type) and $Dhh^{Cre}::Gpr126^{fl/fl}$ ($Gpr126^{\Delta Schwann}$) mice. $Gpr126^{fl/fl}$ nerves were well myelinated (*N* = 3/3 animals), whereas $Gpr126^{\Delta Schwann}$ nerves exhibited myelin loss with readily apparent onion bulb-like structures (arrowheads) (*N* = 3/3 animals). Right panels: Transmission electron

micrographs from *Gpr126*$^{fl/fl}$ and *Gpr126*$^{\Delta Schwann}$ sciatic nerves. Myelinated axons ("M") and Remak bundles ("R") were found in *Gpr126*$^{fl/fl}$ sciatic nerves (*N* = 3/3 animals). Numerous defects were observed in *Gpr126*$^{\Delta Schwann}$ sciatic nerves (*N* = 3/3 animals) including onion bulbs (black arrowheads), abnormal cytoplasmic protrusions (white arrows), and loss of axon-Schwann cell interactions (boxes) similar to *Prnp*$^{ZH3/ZH3}$ mice. Scale bars = 20 μm (a-b), 2 μm (c-d). **C**: *gpr126*^{st63} hypomorphic mutant larvae were treated with vehicle (DMSO) or FT_{23-50} (20 μM) at 50-55 hours post fertilization (hpf) and posterior lateral line nerve was immunostained at 5 days post fertilization (dpf) for myelin basic protein (Mbp, green). AcTub: acetylated tubulin (red) labeling axons. Scale bar = 20 μm. The intensity of immunofluorescence was assessed by morphometry (right graphs). FT treatment enhanced Mbp immunofluorescence without affecting AcTub**. D**: Mbp expression was scored in larvae treated with FT_{23-50} or vehicle (DMSO). FT_{23-50} treatment resulted in a higher proportion of rescued ("some" and "strong") MBP expression in *gpr126*^{st63} (53% vs. 34%), but not in *gpr126*^{st49} larvae ($p < 0.05$, Fisher's two-tailed exact test). N.S. = not significant. $N \geq 25$ larvae per replicate treatment. **E**: *Prnp*$^{ZH3/ZH3}$ and BL6 mice were intravenously exposed to either FT_{23-50} or its non-charged analogue $FT^{K\rightarrow A}_{23-50}$ (600 μg/animal, 20 min). *Prnp*$^{ZH3/ZH3}$ sciatic nerves showed a significant cAMP increase after injection of FT_{23-50}, but not of $FT^{K\rightarrow A}_{23-50}$. FT_{23-50}-treated *Prnp*$^{ZH3/ZH3}$ sciatic nerves reached cAMP levels similar to those of BL/6 mice injected with $FT^{K\rightarrow A}_{23-50}$. Each dot represents an individual animal. **F**: Heart cAMP levels were also increased in FT_{23-50}-injected mice.. **G**: Control *Gpr126*$^{fl/fl}$ (WT) and *Dhh*^{Cre}*::Gpr126*$^{fl/fl}$ mutant (*Gpr126*$^{\Delta Schwann}$) mice were intravenously injected with either FT_{23-50} or uncharged FT_{23-50} ($FT^{K\rightarrow A}_{23-50}$) (600 μg/animal). Sciatic nerves were isolated 20 min post injection. FT_{23-50} elicited a significant cAMP increase in WT mice, but not in *Gpr126*$^{\Delta Schwann}$ mice. $FT^{K\rightarrow A}_{23-50}$ injection did not alter cAMP levels (*N=3*).

Extended Data

Table S1: Sequences of synthetic peptides used in the present study. The collagen-4 homology domain necessary for cAMP induction is highlighted in yellow.

Name	Sequence
FT_{23-50}	KKRPKPGGWNTGGSRYPGQGSPGGNRYP
FT_{23-50}-HA	KKRPKPGGWNTGGSRYPGQGSPGGNRYPYPYDVPDYA
FT_{34-69}-HA	PGQGSPGGNRYPPQGGTWGQPKGGGWGQYPYDVPDYA
FT_{51-94}-HA	PQGGTWGQPHGGGWGQPHGGSWGQPHGGSWGQPHGGGW
FT_{83-109}-HA	PHGGGWGQGGGTHNQWNKPSKPKTNLKYPYDVPDYA
FT_{94-110}-HA	GGGTHNQWNKPSKPKTNLKHYPYDVPDYA
FT_{94-110}	GGGTHNQWNKPSKPKTNLKH
AlaQGSPG	KKRPKPGGWNTGGSRYPGAAAAAGNRYP
AlaKKRPK	AAAPAPGGWNTGGSRYPGQGSPGGNRYP
ColIV	GPRGKPGVDGYNGSRGDPGYP
ColIV-Mut	AAAGAAGVDGYNGSRGDPGYP
FT_{23-34}	KKRPKPGGWNTG
SFT_{23-34}	AAAGAAGGWNTG

Supplementary Figure Legends

Figure S1. A: Primary Schwann cells were isolated from the sciatic nerves of *Prnp*$^{ZH1/ZH1}$ mice and grown on coverslips. Cells were exposed for 20 min to recombinant PrP^{C}, FT, or GD (2µM), fixed, and stained with POM2 (FT, PrP^{C}) or POM1 (GD). Antibodies were visualized in the green channel and nuclei were stained with DAPI (blue). PrP^{C} and FT, but not GD, adhered to the cells. Scale bars: 25µm **B**: Schematic representation of the target region for transcription activator-like endonucleases (TALEN) in the *Prnp* gene. Target guides are indicated by arrows. Gene editing resulted in a deletion leading to a frame shift in the PrP^{C} coding sequence (designated as conflict in the figure) and a premature stop codon identified by sequencing. **C:** Wild-type SW10 cells and a subclone isolated after treatment with TALEN (termed SW10$_{\Delta PrP}$) were probed by Western blotting using anti-PrP antibody (POM1). SW10$_{\Delta PrP}$ showed complete abrogation of PrP^{C} expression and was used for further experiments. Levels of actin on the same membrane were monitored to confirm equal loading of cell lysates onto the gel. **D-E**: SW10$_{\Delta PrP}$ cells were treated with full-length recombinant (PrP^{C}, residues 23-231), flexible tail (FT, 23-110), or globular domain (GD, 121-231). PrP epitopes were detected with POM2 (D) or POM1 (E) (red). Grey: DAPI. As expected, FT was detected only by POM2. Cells were also labeled with antibodies to the p75 nerve-growth factor receptor (yellow), a Schwann cell marker. PrP^{C} and FT, but not GD, adhered to Schwann cells. Scale bar: 26 µm. **F**: the PrP^{C}-deficient cell line HpL[5] was treated with recombinant PrP^{C}, FT, and GD as in panel A. None of the recombinant proteins adhered to HpL cells. Scale bars: 20 µm. **G:** SW10 cells were trypsinized, washed, and mixed with non-trypsinized SW10 cells labeled with Deep Red cell tracker. Cells were incubated with HA-tagged peptide FT$_{23-50}$, and binding was visualized by flow cytometry. The Deep red signal (abscissa) was used to differentiate trypsinized from non-trypsinized cells. 51% of untreated cells, but only 5% of trypsinized cells, became decorated by FT$_{23-50}$-HA, indicating that FT$_{23-50}$ reacted with trypsin-sensitive surface molecules. **H**: SW10 cells were digested (30 min) with phosphatidylinositol phospholipase C (PI-PLC, 0.5 units), washed, and incubated with FT$_{23-50}$-HA along with undigested Deep-Red labeled cells (left panel). The proportion of binders in the digested (34%) and the undigested samples (30%) was similar, indicating that the FT$_{23-50}$ receptor was neither PrP^{C} itself nor any other GPI-linked protein. To monitor the efficiency of PI-PLC treatment, we assessed POM2 binding to PrP^{C} on both treated and untreated cells (right

panel). POM2 binding was significantly decreased in PI-PLC treated cells (23%) compared to untreated cells (90%).

Figure S2. A-B: cAMP was measured in sciatic nerves isolated from 4-day old (A) or 4-week old (B) BL6 and *Prnp*$^{ZH1/ZH1}$ mice. No difference was observed in cAMP levels in 4-day old mice, whereas 4-week old *Prnp*$^{ZH1/ZH1}$ mice displayed a trend towards decreased cAMP levels. **C**: Sciatic nerve from 10-week old *Prnp*$^{ZH3/ZH3}$ mice showed a significant decrease in cAMP ($p= 0.0151$). **D**: SW10 cells were seeded in 6 well plates and treated (20') with recombinant FT or GD (10 µM). Addition of FT, but not of GD, resulted in a concentration-dependent intracellular cAMP increase.

Figure S3. **A**: HEK293T cells were transfected with an empty vector (HEK^{empty}) or a plasmid expressing murine PrP^{C} (HEK^{PrP}). Cell medium was collected 48h after transfection and subjected to immunoprecipitation with monoclonal antibody POM2 (against PrP^{C}), followed by western blotting using biotinylated POM2 and streptavidin-HRP. FT was observed only in the medium from HEK^{PrP} cells. **B**: FT released into the conditioned medium of HEK^{PrP} was immunoprecipitated using POM2 and visualized by Western blotting with biotinylated POM2. Dilutions of recombinant FT (3.125 - 100 ng) were used for calibration, and the concentration of FT released into the medium was estimated at 37 ng/ml. **C:** Conditioned medium from primary BL6 Schwann cells cultures (PSC^{BL6}) was subjected to immunoprecipitation with antibody POM2 (against PrP^{C}) followed by Western blotting with POM2. For control, we used conditioned medium from HEK cells transfected with a non-coding plasmid (HEK^{empty}) or a with a plasmid encoding murine PrP^{C} (HEK^{PrP}). FT was only detected in conditioned medium from HEK^{PrP} cells (lane 2) but not in conditioned medium from two independent PSC^{BL6} cultures (lanes 3-4). Asterisks denote immunoglobulins detected by the secondary antibody. **D:** Sciatic nerves lysates obtained from 10 week old *Prnp*$^{ZH1/ZH1}$ and BL6 mice and subjected to immunoprecipitation with POM2 antibody followed by Western blotting with POM2. Full length PrP^{C}, but no FT, was detectable in the immunoprecipitates from BL6 mice. **E:** Wild-type HEK293T cells (HEK^{WT}) or HEK293T cells overexpressing various GPCRs bearing V5 epitope tags (HEK^{Gpr126}, HEK^{Gpr124}, and HEK^{Gpr176}) were grown on coverslips and stained with anti V5 antibody (detecting tagged GPCRs; magenta). Nuclei were stained with DAPI (blue). Staining revealed cell surface

expression of all transfected GPCRs. Scale bar: 8µm. **F:** Binding of HA-tagged FT_{23-50} to HEK^{GPR126} cells (right panel, monitored by cytofluorimetry) was conspicuously increased over that of wild-type, Gpr176, and Gpr124-overexpressing HEK293T cells.

Figure S4. A: HEK293T, HEK^{GPR124} and HEK^{GPR126} cells were exposed (20 min) to recombinant FT, GD (2µM), or PBS, and subjected to immunoprecipitation using the anti-V5 antibody, followed by Western blotting using POM2, anti-V5 or POM1. Anti-V5 detected both full-length Gpr126, Gpr124 (denoted as GprV5 for both proteins) and the respective C-terminal fragments (Gpr126V5-CTF, Gpr124V5-CTF). POM2 revealed a band corresponding to the FT (lane 3) that co-precipitated with GPR126. POM1 indicated that GD did not bind. Lanes 1, 2 and 3: HEK^{GPR126} cells treated with PBS, GD and FT. Lanes 4, 5 and 6: HEK^{GPR124} cells treated with PBS, GD and FT. Lanes 7, 8 and 9: HEK293T cells treated with PBS, GD and FT Asterisks: immunoglobulin heavy and light chains. **B**: $SW10_{\Delta Gpr126}$ cells plated at a density of 100'000 cells/well in 6-well plates were transfected with control plasmid (pCDNA3) or plasmids encoding various GPCRs (Gpr126, 124, 176, and 56) bearing C-terminal V5 tags. Only cells transfected with pCGpr126-V5 showed a cAMP response to FT_{23-50} 48h post transfection. PBS treatment was used for control. **C:** Intracellular cAMP responses to FT treatment (2 µM, 20') in SW10 and $SW10_{\Delta Gpr126}$ cells, as well as $SW10^{huGpr126}_{\Delta Gpr126}$ cells expressing V5-tagged human Gpr126 (pCGpr126-V5). A significant increase in cAMP was observed in SW10 cells, whereas $SW10_{\Delta Gpr126}$ showed no change. In contrast, $SW10^{huGpr126}_{\Delta Gpr126}$ cells showed a significant cAMP increase, indicative of successful complementation. **D:** SW10 and $SW10_{\Delta Gpr126}$ cells were grown on coverslips for 24h and exposed to recombinant FT (2 µM, 20 min). Cells were stained with POM2 (detecting FT; red, DAPI-stained nuclei: grey) and antibodies to $p75^{NGFR}$ (yellow). Deletion of Gpr126 largely suppressed FT binding. Scale bar: 26 µm. **E**: HEK293(H) cell lines were transfected with plasmids expressing different adhesion GPCRs (Gpr: 97, 133, 64, 56), followed by selection of cells expressing the receptor in presence of geneticin. GPCR expressing cells and HEK^{Gpr126} cells were then treated with either FT_{23-50} or $FT^{K\rightarrow A}_{23-50}$ for control (FT and C, respectively). Only cells expressing Gpr126 responded to FT_{23-50} with a cAMP spike. Interestingly, cells expressing Gpr133 reacted with a decrease in

cAMP levels. **F:** HEK293T cells were transfected with increasing amounts of human Gpr126 plasmid (2-5µg/well of a 6 well plate). 48h post transfection cells were treated with FT_{23-50} or PBS as a control. Increasing amount of Gpr126 cDNA did not result in amplification of cAMP signal.

Figure S5. A: Primary *Prnp*$^{ZH1/ZH1}$ cerebellar granule neuron cultures were seeded in 6-well plates at a density of $5x10^5$ cells and treated with FT_{23-50}, $FT^{K\rightarrow A}_{23-50}$, or PBS. No alterations in the levels of cAMP were noticed. **B:** SW10 cells were exposed to conditioned medium from HEK cells that had been transfected with empty vector (HEK^{empty}) or a PrP^C expression vector (HEK^{PrP}). HEK^{PrP} were optionally treated with 100 µM of the TAPI-2 protease inhibitor for 24h before harvesting the medium. TAPI-2 treatment resulted in reduced cAMP induction, suggesting that impaired proteolytic cleavage of the FT from PrP^C resulted in decreased signaling. **C:** Quantification of FT released into the medium relative to the total amount of PrP^C in lysates by Western blotting. The spent medium of HEK^{PrP} cells treated with TAPI-2 contained less FT. **D**: SW10 and $SW10_{\Delta Gpr126}$ cells were transfected with an Egr2-controlled firefly luciferase reporter and treated with recombinant FT (2µM) or PBS (24 hrs). Ordinate: luciferase expression normalized to a renilla luciferase control (n=3; *: $p<0.05$; t-test). Luciferase activity was observed only in SW10 cells stimulated with FT but not in $SW10_{\Delta Gpr126}$ cells. **E:** Primary Schwann cells were exposed to recombinant FT (2 µM, 1h) or PBS. Egr2 mRNA expression was measured by quantitative RT-PCR and normalized against a panel of housekeeping genes. **F**: $SW10_{\Delta PrP}$ and $SW10_{\Delta Gpr126}$ cells were grown in 6-well plates, exposed to recombinant FT (≤30 min), and analyzed by Western blotting (left). Densitometry (right) showed increased phospho-AKT/AKT ratio in $SW10_{\Delta PrP}$ cells, but not in $SW10_{\Delta Gpr126}$ cells.

Figure S6. A: SW10, $SW10_{\Delta PrP}$ and $SW10_{\Delta Gpr126}$ cells were grown on coverslips and stained with antibodies against Myelin associated glycoprotein (MAG), Myelin oligodendrocyte glycoprotein (MOG), glial fibrillary acidic protein (GFAP) and p75 nerve growth factor receptor (p75NGFR) (left panel, all green; DAPI-stained nuclei: blue). Cells labeled with secondary antibody alone (2° Ab) were used as control to determine unspecific staining. Scale bars: 10µm. Expression in all cell lines was confirmed by western blotting (right panel). Lysate from HEK293T wild-type cells (HEK^{WT}) was used as control. All proteins

except Myelin basic protein (MBP) were expressed in SW10 cells and its derivatives. **B:** Western blot (developed with POM2) of HEK 293T cells transfected with expression plasmids for wild-type murine PrP^C or for PrP^C bearing lysine-to-alanine substitutions in the KKRPK and QGSPG motifs (lanes 3 and 4, respectively). The mutations did not affect the biogenesis and processing of PrP^C **C:** Western blot of the medium collected from the cells shown in panel B. FT fragments bearing the mutations were released into the medium similarly to wild-type FT. **D:** $SW10_{\Delta PrP}$ cells were treated with conditioned medium from HEK293T cells transfected with an empty vector (HEK^{empty}), with PrP^C (HEK^{PrP}), or with full-length PrP^C versions in which the QGSPG ($HEK^{PrP\sum QGSPG}$) or KKRPK ($HEK^{PrP\sum KKRPK}$) motifs were substituted (∑) with alanines. The charge neutralization within the KKRPK motif abrogated the cAMP induction. **E**: $SW10_{\Delta PrP}$ cells were treated with FT_{23-50} (2 µM) or a Col4-derived 21-meric synthetic peptide containing either the GPRGKPG domain or its alanine-substituted variant (AAAGAAG; both 8 µM). Both FT_{23-50} and the native Col4 peptide, but not the alanine-substituted peptide (Ala-Col4), induced cAMP.

Figure S7. A: Transmission electron micrographs of 14 month-old $Prnp^{ZH1/ZH1}$ sciatic nerves (ZH1). Black arrowhead: thinly myelinated axons; white arrowhead: abnormal cytoplasmic Schwann cell protrusions; boxes: loss of axon-Schwann cell interactions; asterisk: initial onion bulb formation. Scale bar: 2 µm in upper left panel; 500 nm in all other panels. **B-C**: Quantification of unmyelinated axons in Remak bundles was performed manually by counting number of axons in the bundles from electron microscopy images (1500x magnification, 10 images per mouse were analyzed and three mice per genotype were used in total). The bundles were further sorted into three categories; <10 axons, 10-20 axons and >20axons/bundle. Comparisons were performed between either BL6 and $Prnp^{ZH3/ZH3}$ (**B**) or $Gpr126^{fl/fl}$ (WT) and $Dhh^{Cre}::Gpr126^{fl/fl}$ ($Gpr126^{\Delta Schwann}$) mice (all mice were 13 month old in age). Both $Prnp^{ZH3/ZH3}$ and $Gpr126^{\Delta Schwann}$ mice showed a similar inclination towards decrease in number of axons per bundle. Statistical significance was established by performing a two-way annova with Bonferroni correction. **D:** Onion bulb like structures were quantified from electron microscopy images (1500x magnification, 10 images per mouse were analyzed and three mice per genotype were used in total) of either BL6 and $Prnp^{ZH3/ZH3}$ or $Gpr126^{fl/fl}$ (WT) and $Dhh^{Cre}::Gpr126^{fl/fl}$ ($Gpr126^{\Delta Schwann}$) mice. These onion bulb like structures were prevalent only in $Prnp^{ZH3/ZH3}$ and $Gpr126^{\Delta Schwann}$ mice, with $Gpr126^{\Delta Schwann}$ exhibiting more.

Figure S8. A: Immunofluorescence for myelin basic protein (Mbp; green) in the posterior lateral line nerve of wild-type zebrafish larvae. AcTub: acetylated tubulin (red) labels the axons. Scale bar = 20 μm. **B:** *gpr126*^{st49} hypomorphic mutant larvae were treated with vehicle (DMSO) or $FT_{23\text{-}50}$ (20 μM) at 50-55 hours post fertilization (hpf) and immunostained at 5 days post fertilization (dpf) for myelin basic protein (Mbp, green). AcTub: acetylated tubulin (red) labeling axons. Scale bar = 20 μm. $FT_{23\text{-}50}$ treatment did not alter Mbp immunofluorescence. **C:** $FT_{23\text{-}50}$ or $FT^{K\rightarrow A}_{23\text{-}50}$ was intravenously administered to *Prnp*$^{ZH1/ZH1}$ and BL6 mice (600 μg/mouse, 20 min). After $FT_{23\text{-}50}$ injection, cAMP levels in *Prnp*$^{ZH1/ZH1}$ mice increased to levels approaching those of BL6 mice. Each dot represents an individual animal. **D:** cAMP spiked also in hearts of $FT_{23\text{-}50}$ injected but not in $FT^{K\rightarrow A}_{23\text{-}50}$ injected mice. *: $p<0.05$; **: $p<0.01$. **C-D:** $FT_{23\text{-}50}$ or $FT^{K\rightarrow A}_{23\text{-}50}$ was injected intravenously into 10-16-week old *Prnp*$^{ZH1/ZH1}$ or BL6 mice (600 μg/animal, 20 minutes). cAMP levels in kidneys (**E**) and brain (**F**) showed no significant changes.

Figure S9-S10: Includes the uncropped blots from different figures in the manuscript. All the images were cropped in Adobe Photoshop and realigned in Adobe Illustrator.

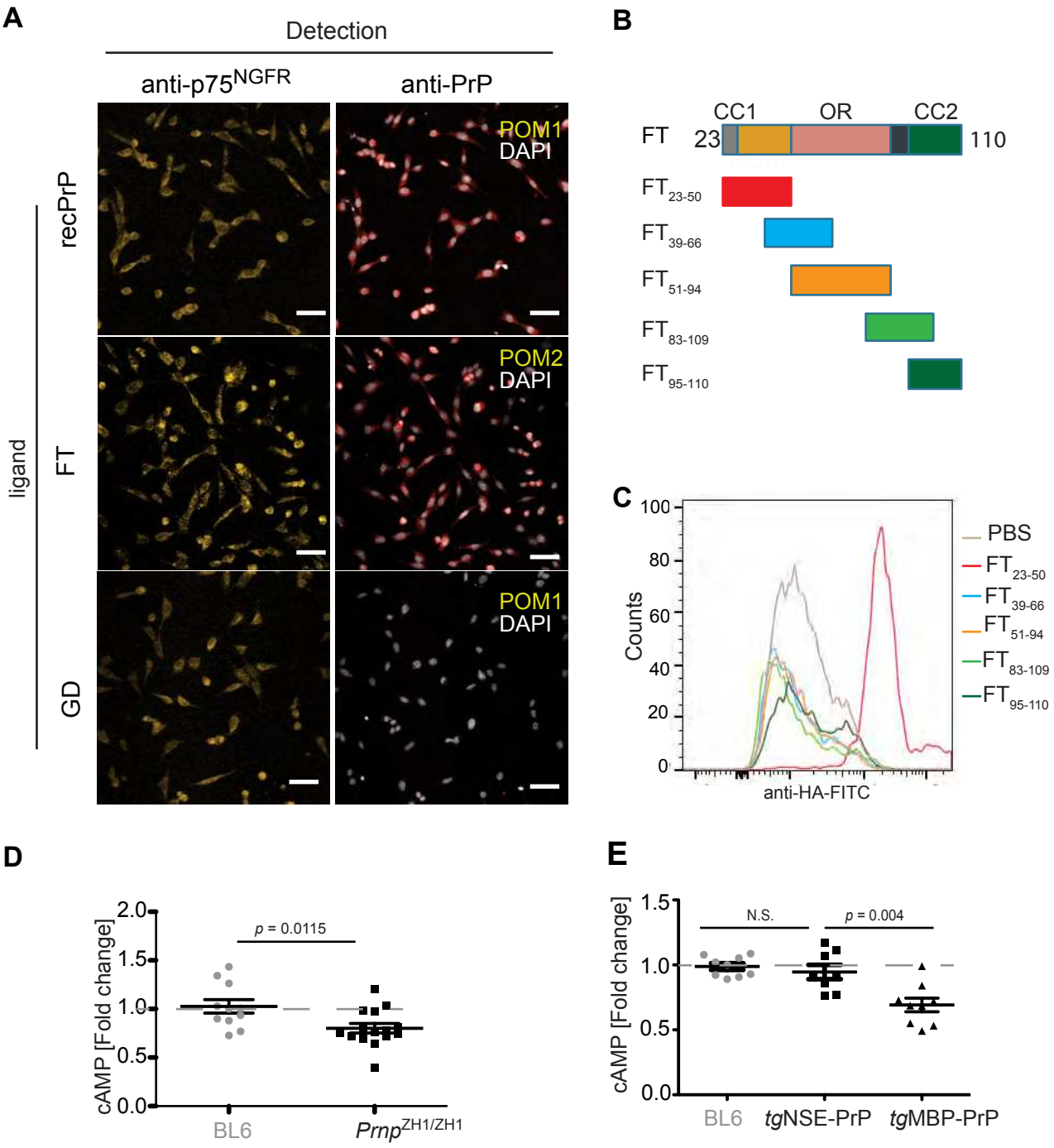

Küffer et al; Fig. 1

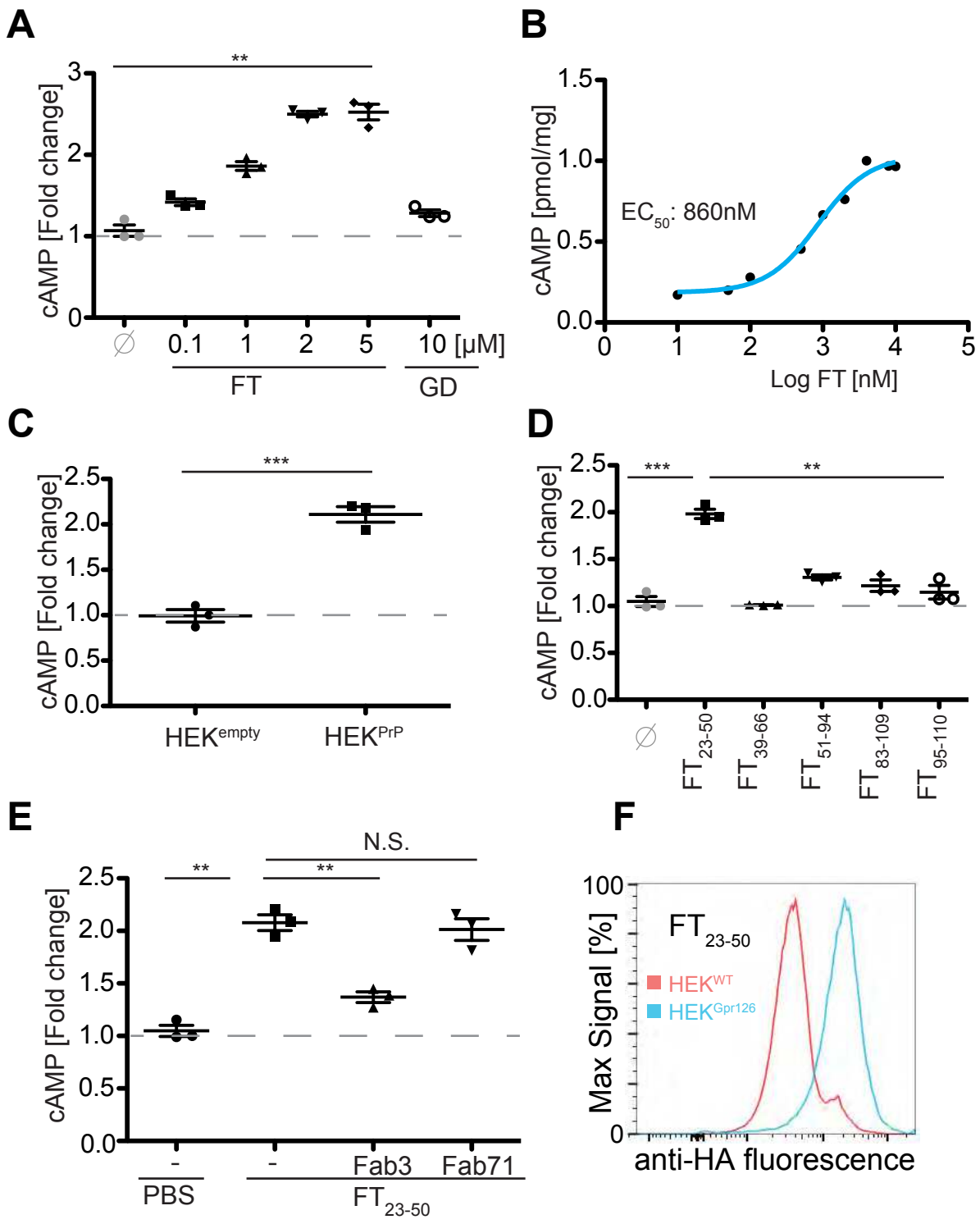

Küffer et al: Fig. 2

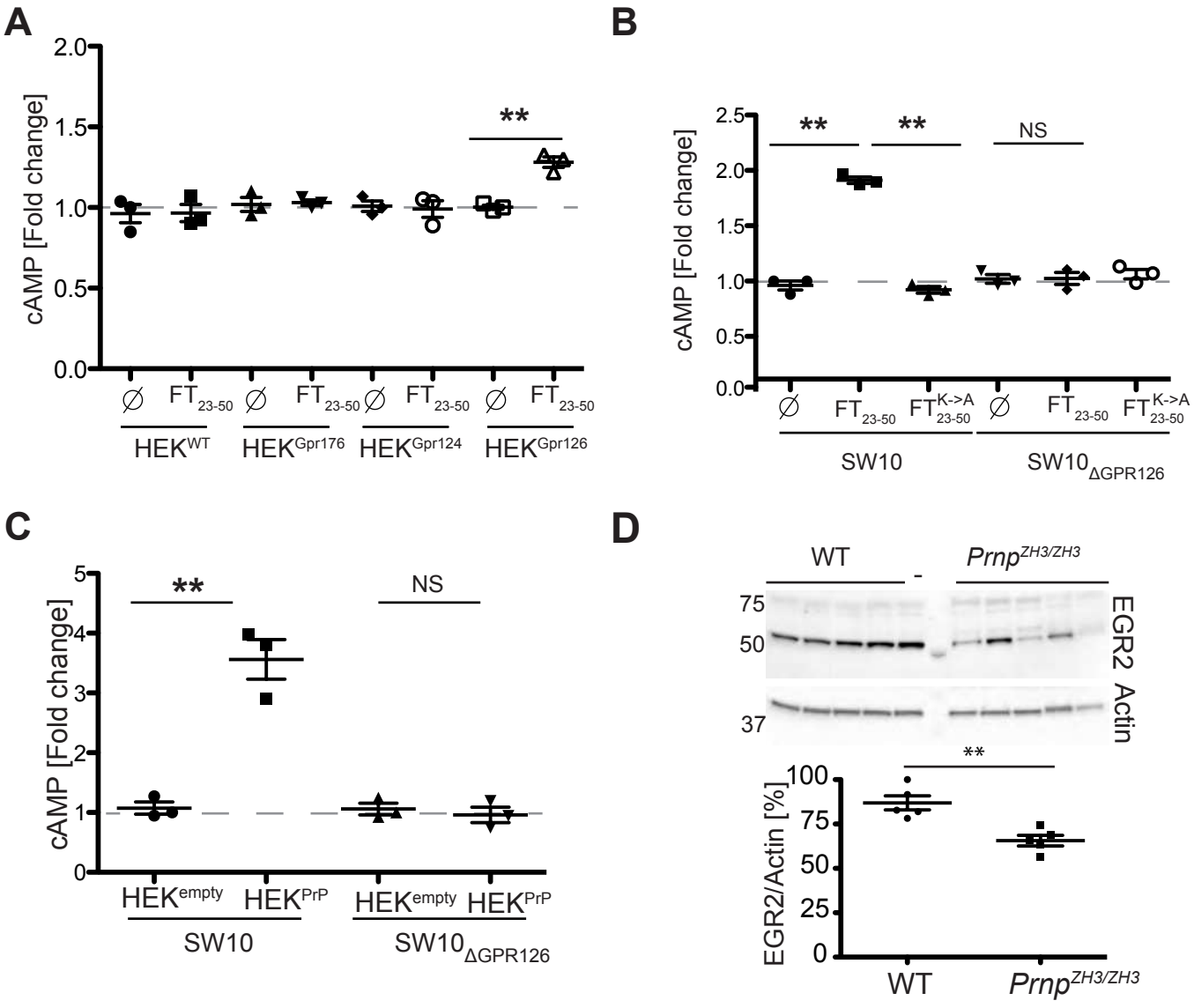

Küffer et al; Fig. 3

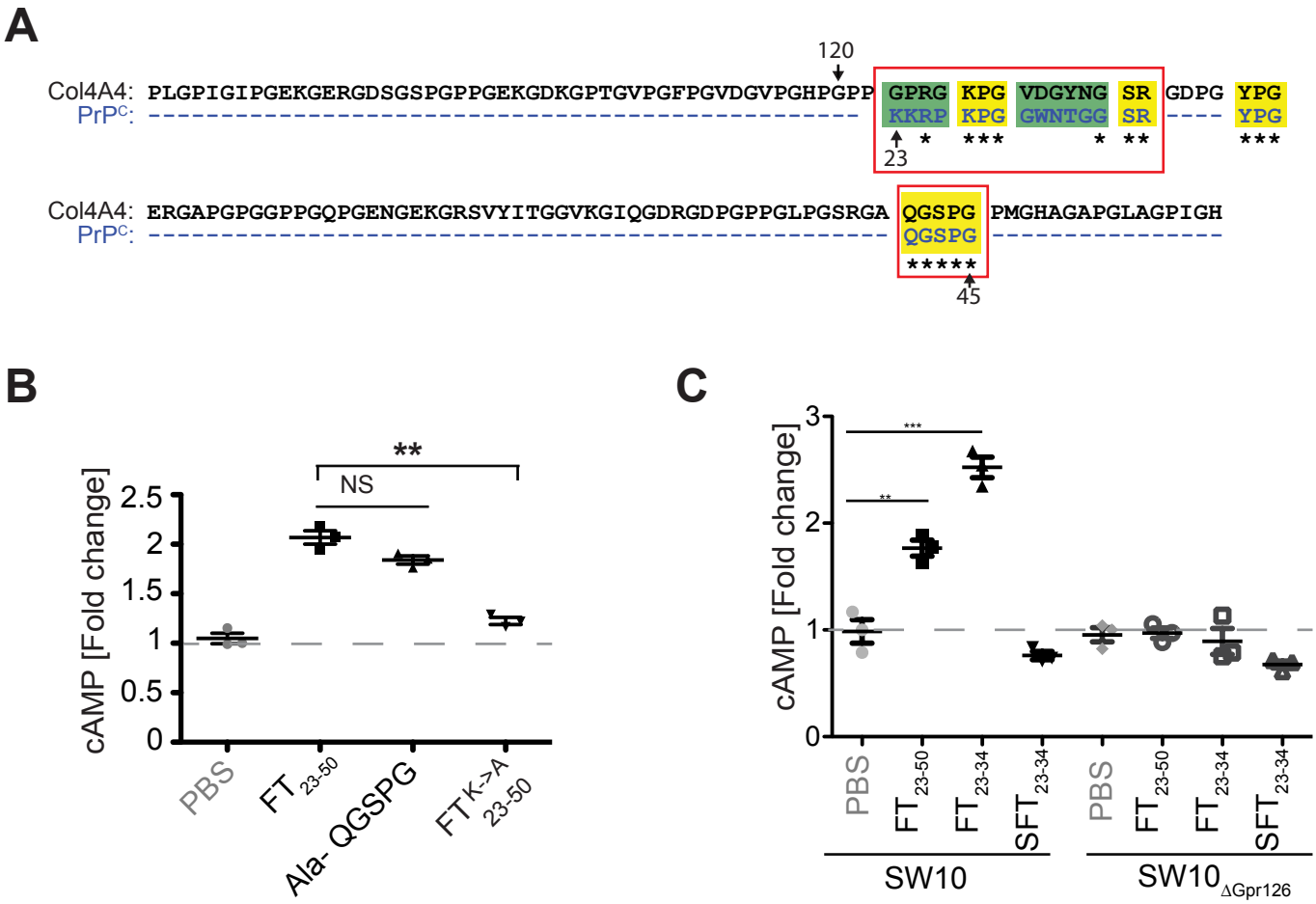

Küffer et al; Fig. 4

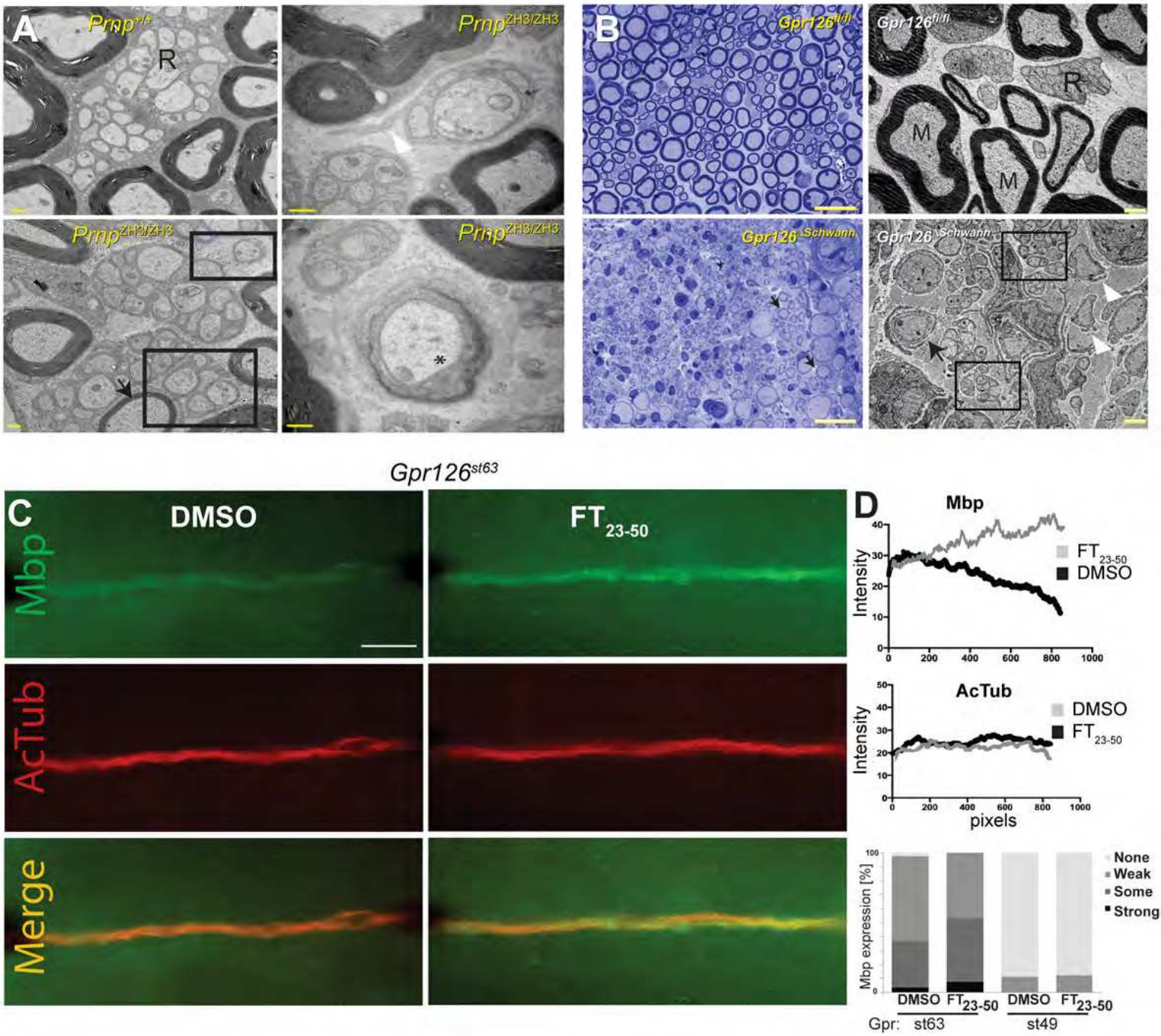

Küffer et al; Fig. 5

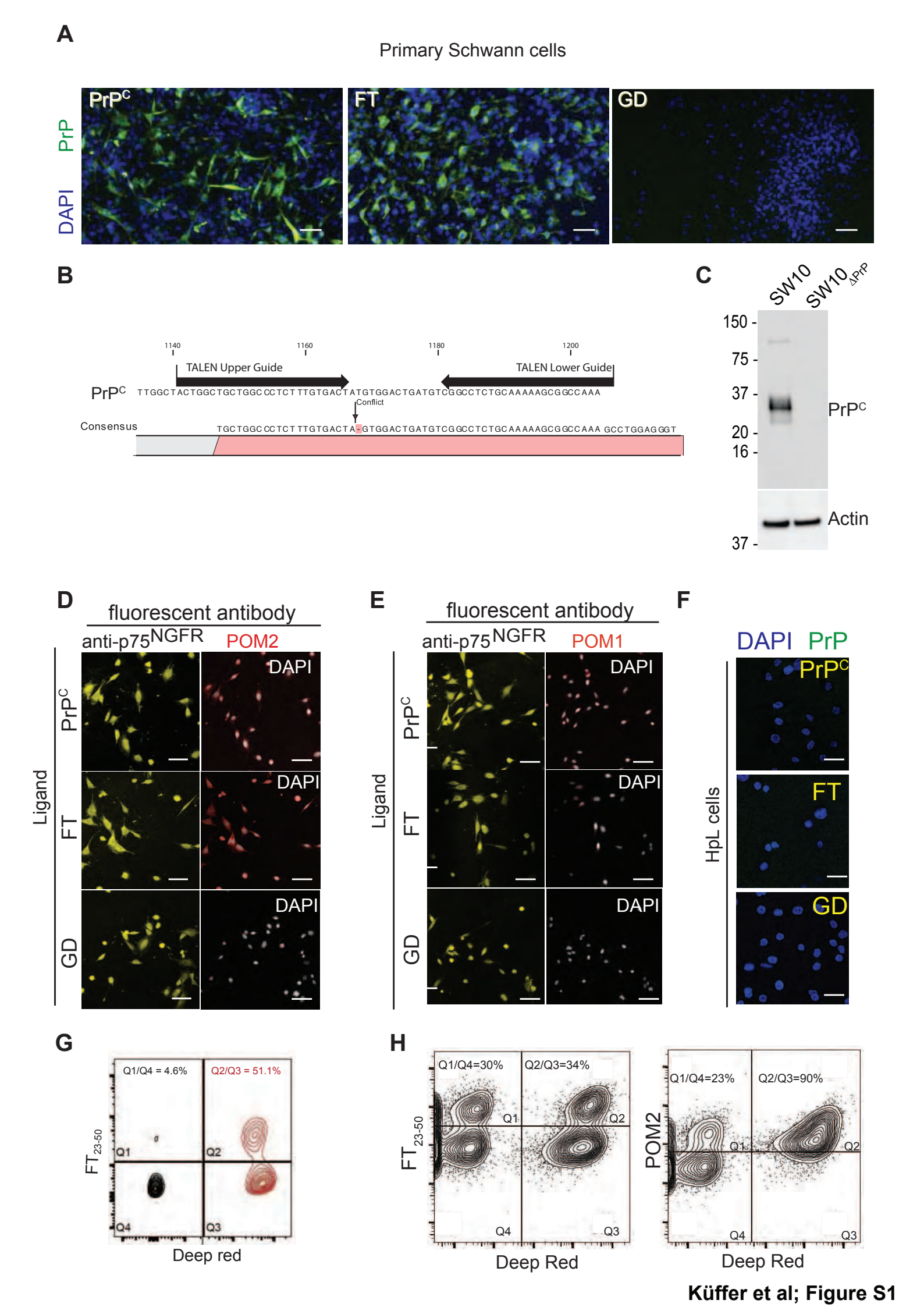

Küffer et al; Figure S1

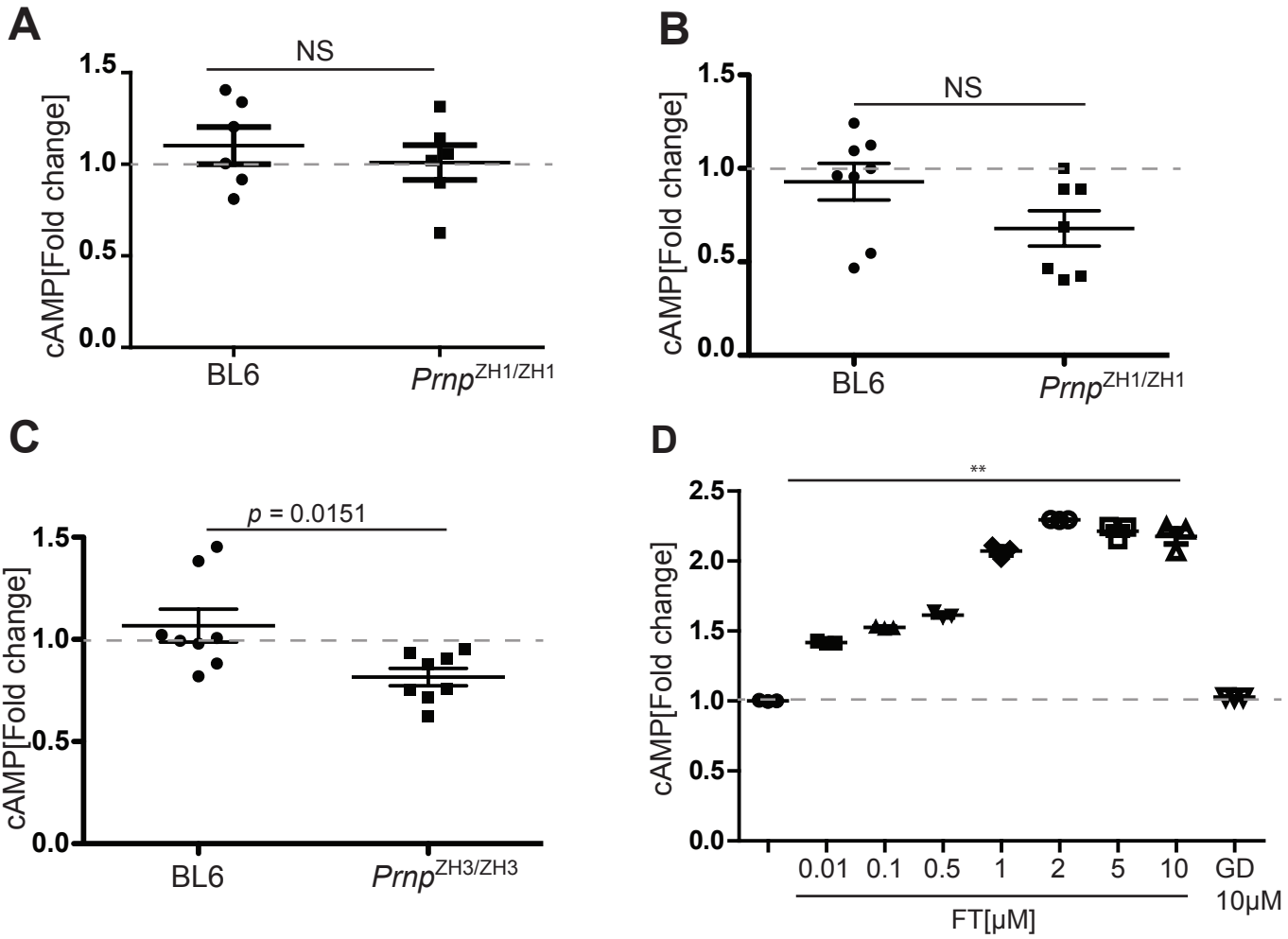

Küffer et al; Figure S2

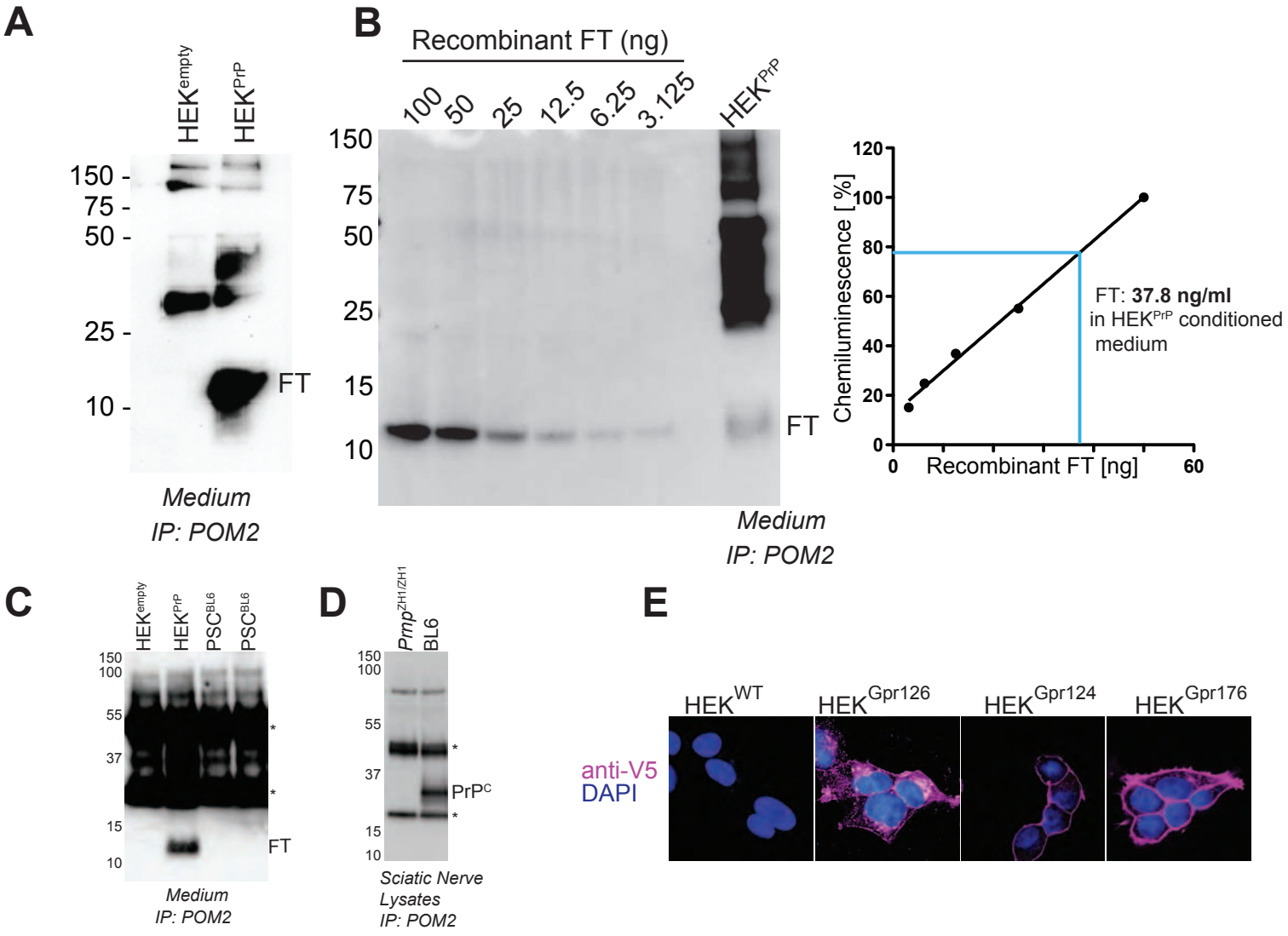

Küffer et al; Figure S3

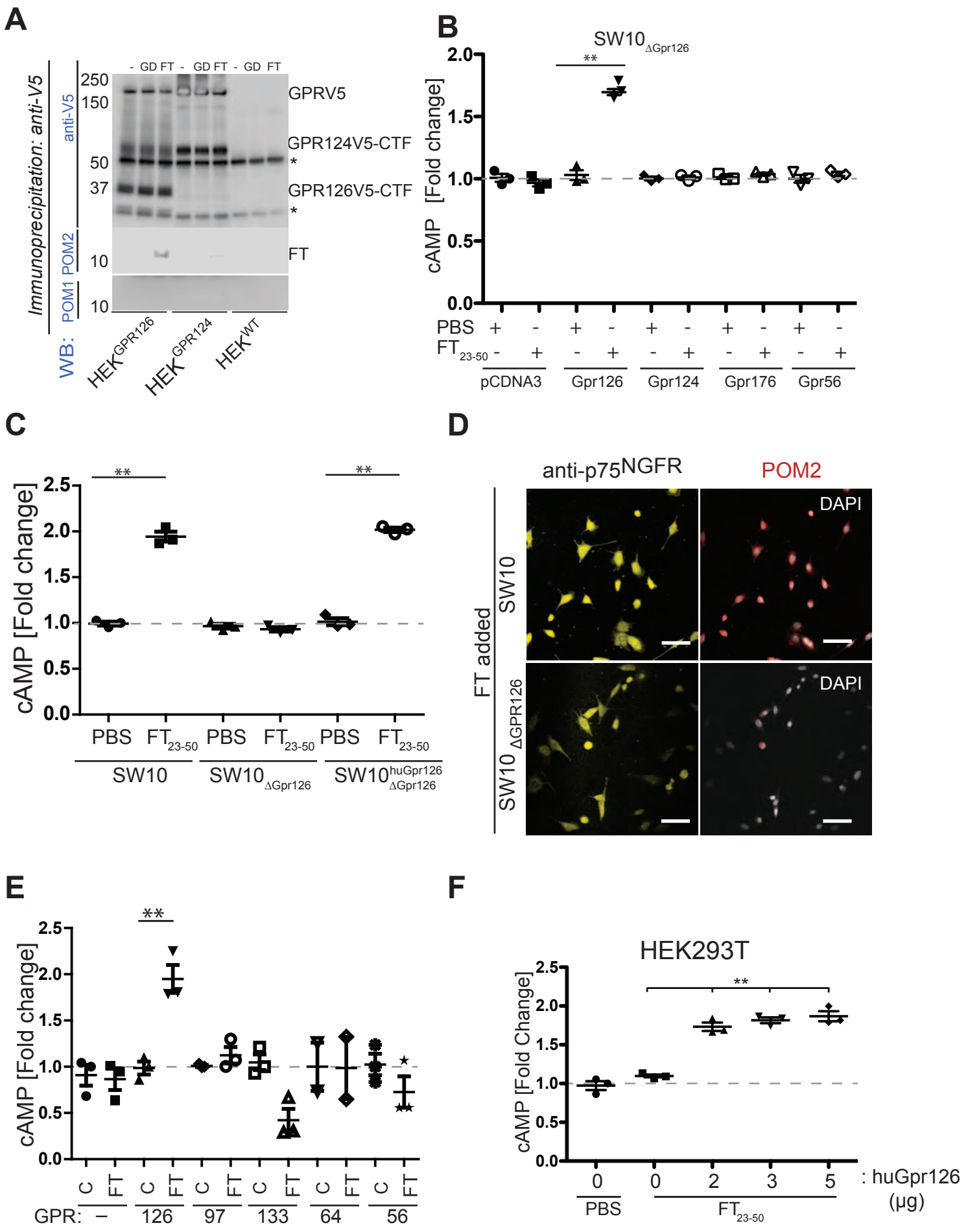

Küffer et al; Figure S4

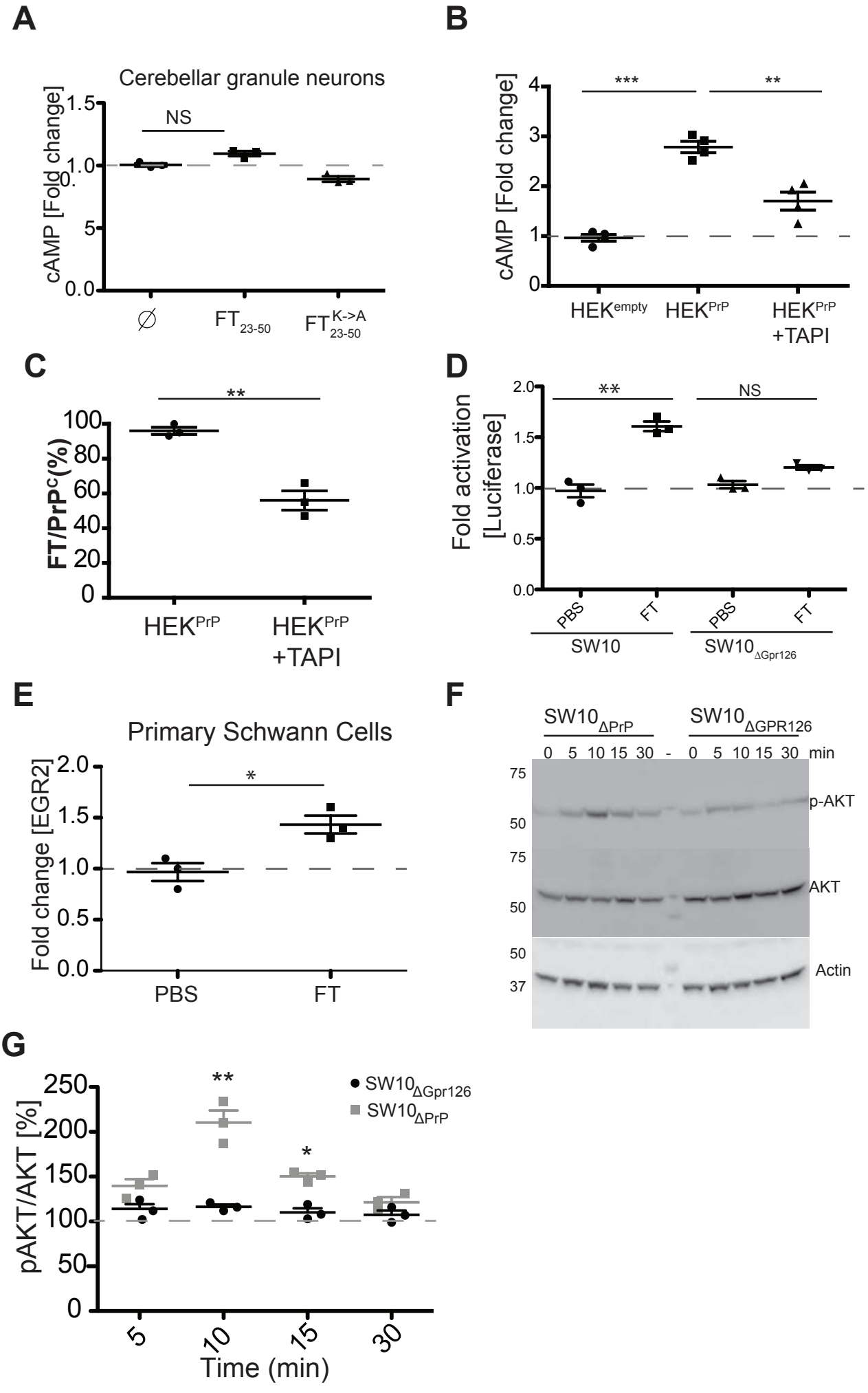

Küffer et al; Figure S5

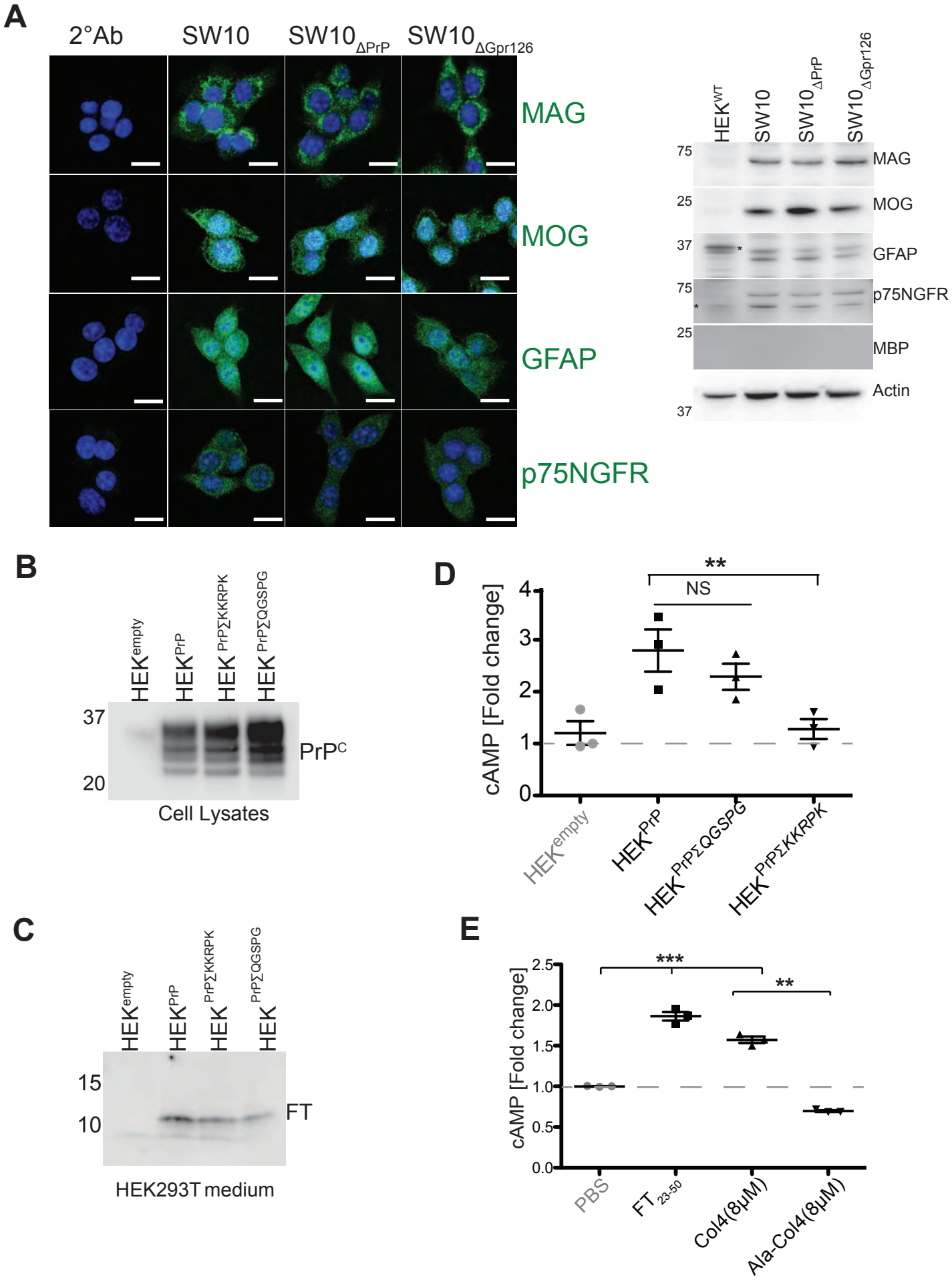

Küffer et al; Figure S6

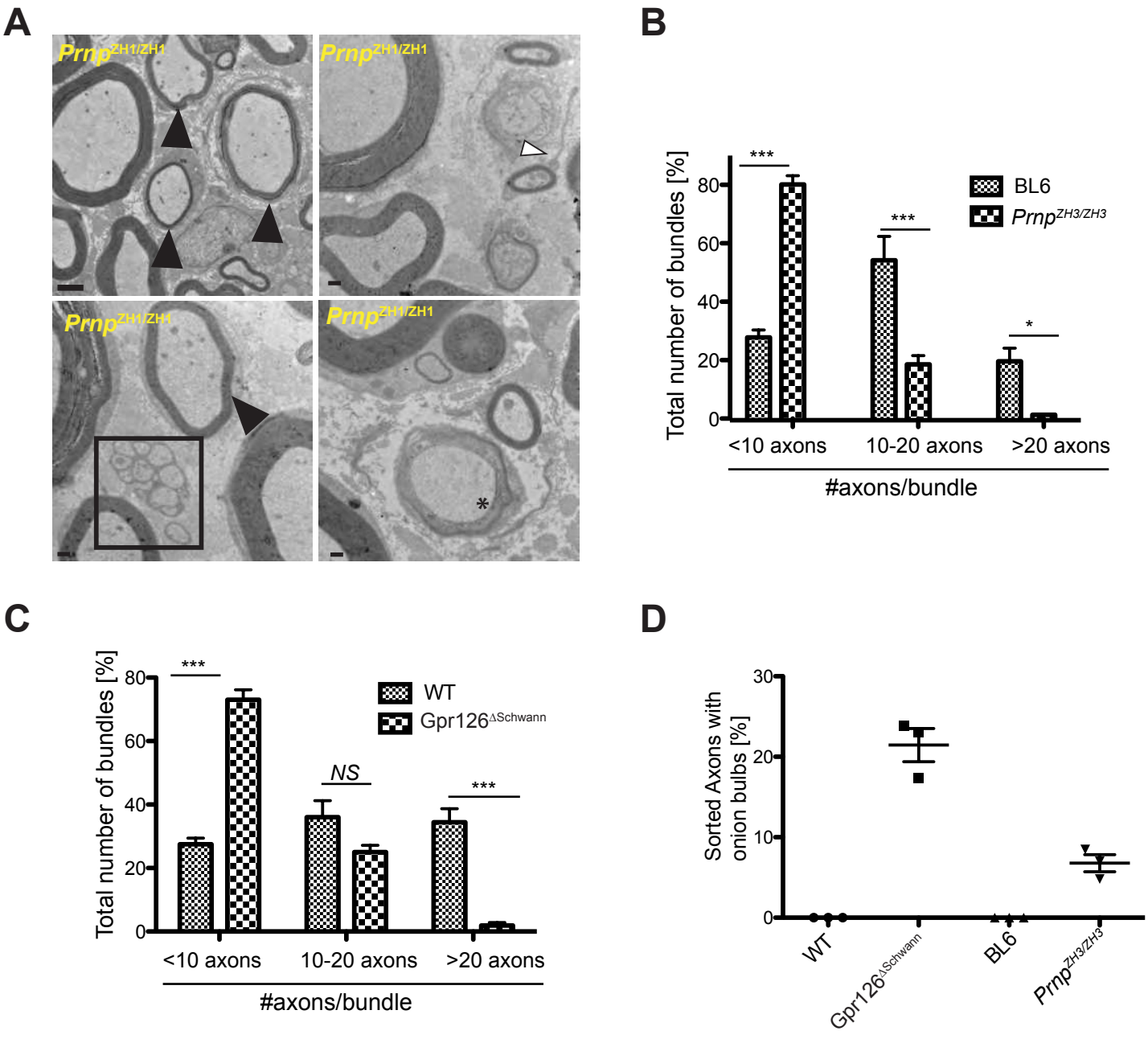

Küffer et al; Figure S7

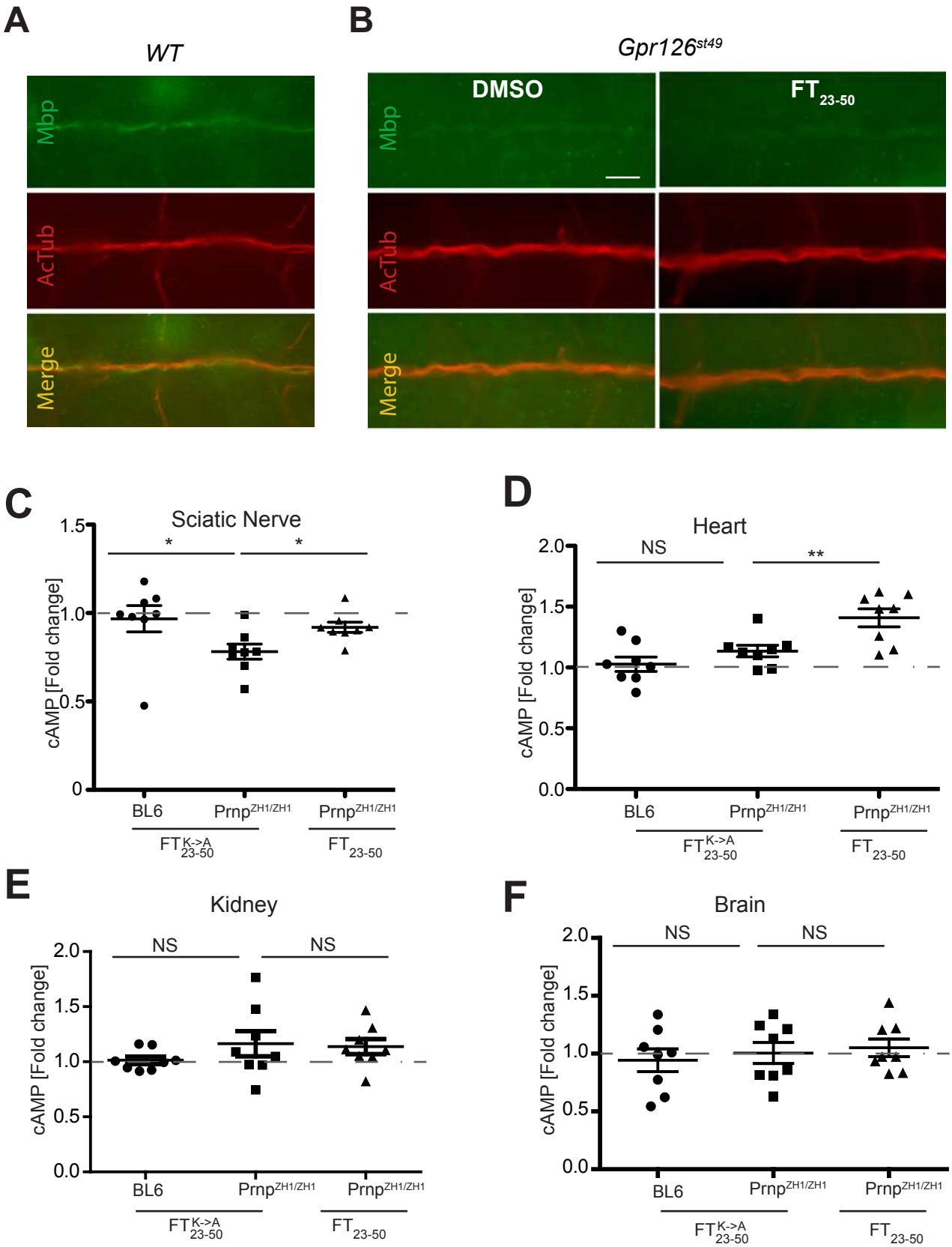

Küffer et al; Figure S8

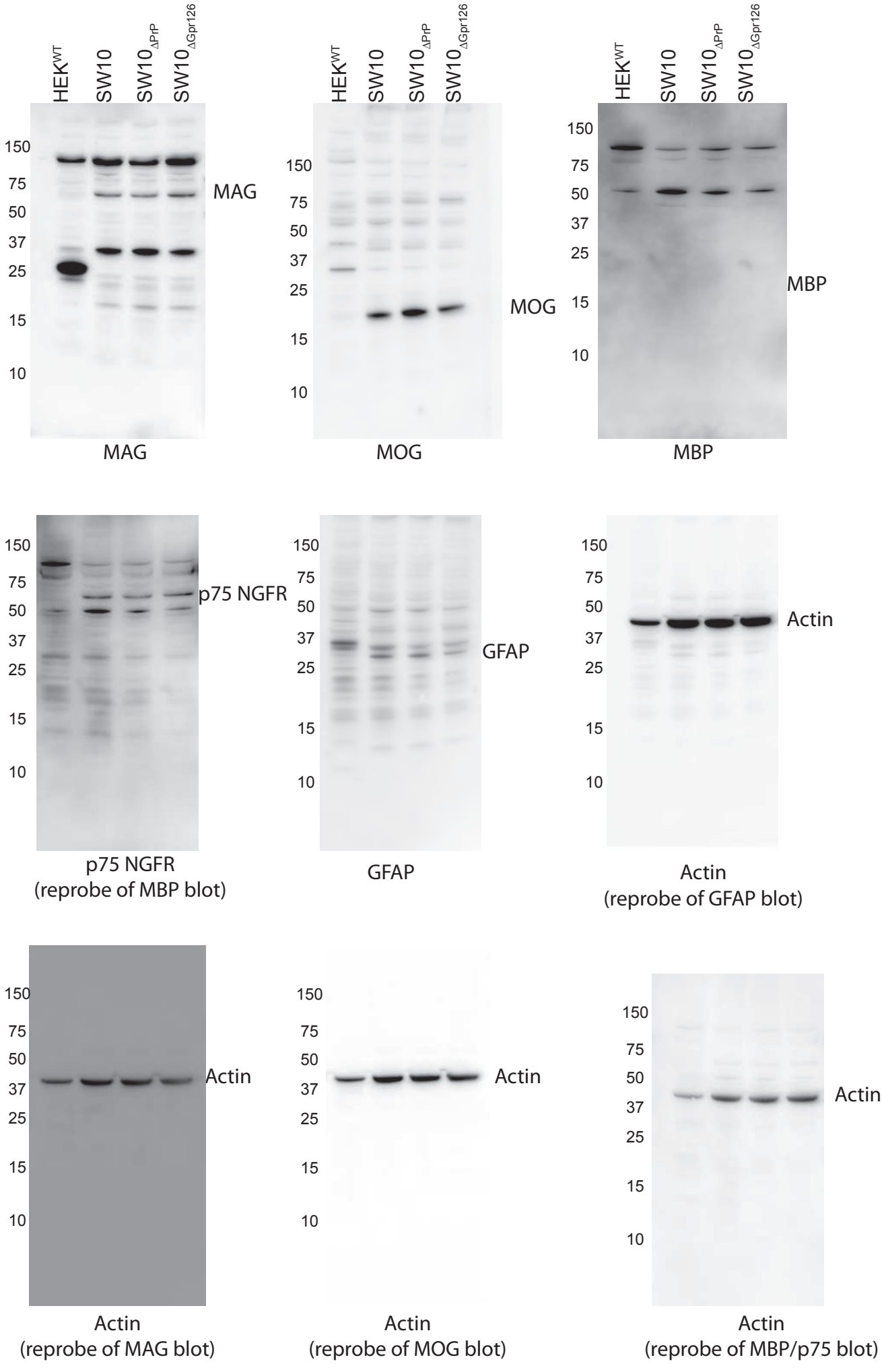
HEK^WT
SW10
SW10_ΔPrP
SW10_ΔGpr126
150
75
50
37
25
15
10
MAG
MOG
MBP
p75 NGFR
GFAP
Actin
Actin
(reprobe of MBP blot)
Actin
(reprobe of GFAP blot)
Actin
(reprobe of MAG blot)
Actin
(reprobe of MOG blot)
Actin
(reprobe of MBP/p75 blot)

Figure S6

Figure S4A: Uncropped Blots

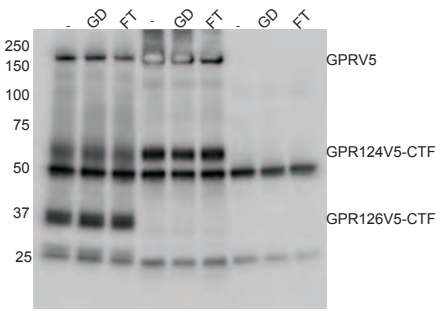

WB: anti V5

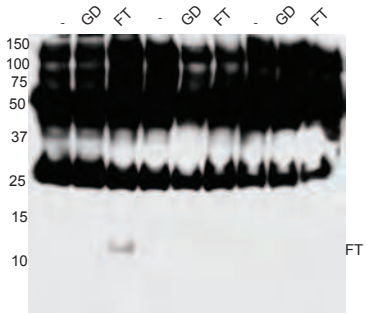

WB: anti POM2

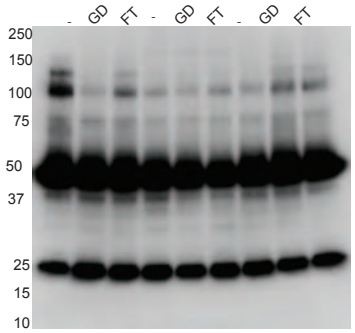

WB: anti POM1

Figure S5F: Uncropped Blots

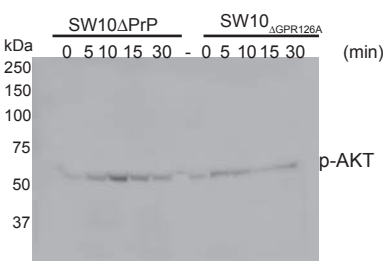

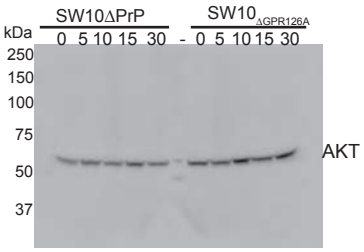

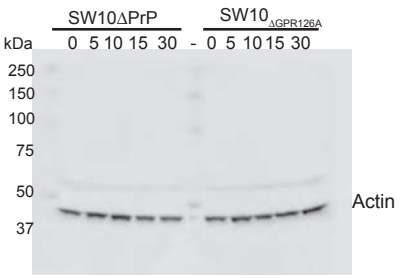

Figure S1C

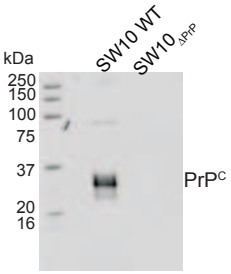

Figure S6B

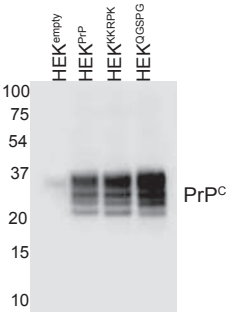

Figure S6C

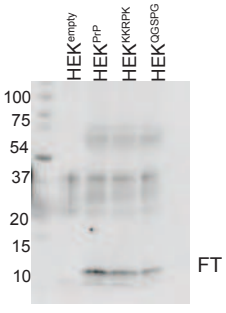

Figure 3D: Uncropped blots

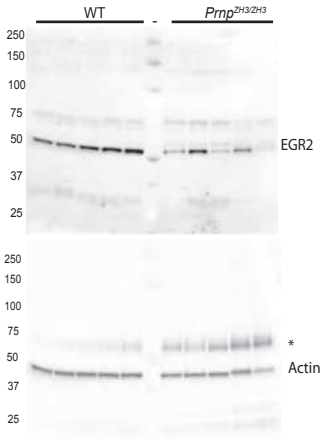

* Non specific band arising from incomplete stripping of the membrane.

- Marker was loaded in the middle lane denoted by -

The membrane was first developed by anti EGR2 antibody followed by stripping the membrane at room temperature followed by reblotting with anti actin antibody.